Exploiting satellite measurements to explore uncertainties in UK bottom-up NO_x emission estimates

~~Exploiting satellite measurements to reduce uncertainties in UK bottom-up NO_x emission estimates~~

Richard J. Pope[1,2], Rebecca Kelly[1], Eloise A. Marais[3], Ailish M. Graham[1], Chris Wilson[1,2], Jeremy J. Harrison[4,5], Savio J. A. Moniz[6], Mohamed Ghalaieny[6], Steve R. Arnold[1] and Martyn P. Chipperfield[1,2]

1: School of Earth and Environment, University of Leeds, Leeds, UK

2: National Centre for Earth Observation, University of Leeds, Leeds, UK

3: Department of Geography, University College London, London, UK

4: Department of Physics and Astronomy, University of Leicester, Leicester, UK

5: National Centre for Earth Observation, University of Leicester, Leicester, UK

6: Department for Environment, Food and Rural Affairs, 2 Marsham Street, London, UK

Submitted to *Atmospheric Chemistry and Physics*

Correspondence to: Richard J. Pope (r.j.pope@leeds.ac.uk)

Abstract

Nitrogen oxides (NO_x, $NO+NO_2$) are potent air pollutants which directly impact on human health and which aid the formation of other hazardous pollutants such as ozone (O_3) and particulate matter. In this study, we use satellite tropospheric column nitrogen dioxide ($TCNO_2$) data to evaluate the spatiotemporal variability and magnitude of the United Kingdom (UK) bottom-up National Atmospheric Emissions Inventory (NAEI) NO_x emissions. Although emissions and $TCNO_2$ represent different quantities, for UK city sources we find a spatial correlation of ~0.5 between the NAEI NO_x emissions and $TCNO_2$ from the high-spatial-resolution TROPOspheric Monitoring Instrument (TROPOMI), suggesting a good spatial distribution of emission sources in the inventory. Between 2005 and 2015, the NAEI total UK NO_x emissions and long-term $TCNO_2$ record from the Ozone Monitoring Instrument (OMI), averaged over England, show decreasing trends of 4.4% and 2.2%, respectively. Top-down NO_x emissions were derived in this study by applying a simple mass balance approach to TROPOMI observed downwind NO_2 plumes from city sources. Overall, these top-down estimates were consistent with the NAEI, but for larger cities such as London and Manchester the inventory is significantly (>25%) less than the top-down emissions.

~~This NAEI NO_x emission underestimate is supported by comparing simulations from the GEOS-Chem atmospheric chemistry model, driven by the NAEI emissions, with satellite and surface NO_2 observations over the UK. This yields substantial model negative biases,~~

~~providing further evidence to demonstrate that the NAEI may be underestimating NO_x emissions in London and Manchester.~~

1. Introduction

Poor air quality (AQ) can have a substantial impact on human health, increasing risk of ailments such as asthma, cancer, diabetes and heart disease (Royal College of Physicians, 2016). A key air pollutant is nitrogen dioxide (NO_2) which was responsible for approximately 9600 premature deaths from long-term exposure in the UK in 2015 (EEA, 2018). NO_2 is also a precursor to tropospheric ozone and nitrate aerosol in the UK (DEFRA, 2018a). Legislation (e.g. the EU directive 2008/50/EC Ambient AQ regulation, (DEFRA, 2018a)) is in place to reduce concentrations of NO_2 and other pollutants. However, many regions in the UK (33 out of 43 in 2019; DEFRA, 2020) still fail to meet the annual mean NO_2 limit of 40 $\mu g/m^3$ (WHO, 2018). To meet the UK's statutory reporting requirements and to help inform policy, Defra uses the National Atmospheric Emissions Inventory (NAEI, 2021). However, like all emission inventories, the NAEI is subject to uncertainties which are difficult to quantify. These uncertainties include unreported sources, diffuse sources such as agriculture, the use of proxy data (e.g. population or housing density data) to distribute emissions and updates to the NAEI methodologies between years (NAEI, 2017). In addition, the NAEI only includes emissions from anthropogenic sources. Spatial verification of the NAEI AQ emissions, until recently (Tsagatakis et al., 2021), has been restricted to comparisons with surface sites, which have limited and disproportional spatial coverage. ~~Spatial verification of NAEI AQ emissions is restricted to comparisons with surface sites, which have limited and disproportional spatial coverage.~~ The NAEI is also used to drive regional models (e.g. the UK Met Office Air Quality in the Unified Model (AQUM, Savage et al., 2013) which provides the official national AQ forecasts), land use regression models (e.g. Wu et al., 2017) and Pollutant Climate Mapping (PCM) models (e.g. Dibbens and Clemens, 2015), where uncertainties in the emissions can then feed into the simulated AQ predictions and resultant public health advisories.

Satellite measurements of tropospheric column NO_2 ($TCNO_2$) have frequently been used to derive top-down emissions of nitrogen oxides (NO_x = nitric oxide (NO) + NO_2), which can be used to evaluate bottom-up inventories. Some studies have used statistical fitting of observed downwind plumes of $TCNO_2$ from anthropogenic sources (e.g. Beirle et al., 2011; Liu et al., 2016; Verstraeten et al., 2018), while others have used complex atmospheric chemistry models deploying approaches such as data assimilation (e.g. Miyazaki et al., 2016), mass balance (Martin et al., 2003) and model sensitivity experiments (e.g. Potts et al., 2021).

While model-derived estimates of NO_x emissions (e.g. from data assimilation) are robust, the methodology is computationally expensive and time intensive. Therefore, the statistical fitting to downwind plumes approach is a more achievable approach to derive top-down emissions, especially for government departments and agencies. Beirle et al. (2011) presented one of the first studies to use statistical fitting to downwind plumes for Riyadh, Saudi Arabia. The method was also applied to multiple megacities and compared with the bottom-up Environmental Database for Global Atmospheric Research (EDGAR) emission inventory (version 4.1). Verstraeten et al. (2018) used a similar, but modified, approach of a simple mass balance which assumes that the observed total mass of NO_2 is a product of the emission rate and the effective lifetime. The assumption is that the removal of NO_2 can be

described by a first-order loss (i.e. the chemical decay of NO_2 follows an exponential decay function with an e-folding time, and therefore distance from source).

In this study, we use satellite $TCNO_2$ records to evaluate the spatial distribution and temporal evolution of the NAEI. In the past, and still presently, this is a challenge given the climatological meteorological conditions (i.e. frequent frontal systems with widespread precipitation and cloud cover; Pena-Angulo et al., (2020)) experienced in the UK. Frequent cloud cover means that satellite instruments are severely restricted in their ability to retrieve information on trace gases and aerosols through the atmosphere (i.e. retrievals only between the top of atmosphere and cloud top). Therefore, the lack of robust observations makes it more difficult to clearly resolve large emission sources from space. Also, previous sensors (e.g. the Ozone Monitoring Instrument, OMI) have had relatively coarse horizontal spatial resolutions (in the order of 10-100 km) which are larger than most UK emissions sources. However, this work represents the first attempt to derive UK city-scale NO_x emissions from the new state-of-the-art TROPOspheric Monitoring Instrument (TROPOMI), which has unparalleled spatial resolution in comparison to previous sensors (e.g. OMI). We apply a similar approach to Verstraeten et al. (2018), but determine the background NO_2 value and e-folding distance in different ways, to derive top-down NO_x emission estimates of UK cities and thereby directly evaluate the NAEI estimates. Therefore, we can derive NO_x emissions from previously undetectable sources (e.g. Manchester and Birmingham). From here on, we refer to this methodology as the simple mass balance approach (SMBA). The satellite observations used, NAEI and SMBA are described in Section 2, the results presented in Section 3 and our conclusions discussed in Section 4.~~I~~

~~n this study, we use satellite $TCNO_2$ records to evaluate the spatial distribution and temporal evolution of the NAEI. We apply a similar approach to Verstraeten et al. (2018), but determine the background NO_2 value and e-folding distance in different ways, to derive top-down NO_x emission estimates of UK cities and thereby directly evaluate the NAEI estimates. This work represents the first attempt to derive UK city scale NO_x emissions from the new state-of-the-art TROPOspheric Monitoring Instrument (TROPOMI), which has unparalleled spatial resolution in comparison to previous sensors (e.g. the Ozone Monitoring Instrument, OMI). Therefore, we can derive NO_x emissions from previously undetectable sources (e.g. Manchester and Birmingham). From here on, we refer to this methodology as the simple mass balance approach (SMBA). The satellite observations used, NAEI and SMBA are described in Section 2, the results presented in Section 3 and our conclusions discussed in Section 4.~~

2. Data and Methods

2.1 NAEI Emissions

The NAEI is the official UK bottom-up inventory of primary sources of emissions, used for statutory reporting, national air quality policy and driving regional air quality models (NAEI, 2021). The contract to deliver the NAEI is led by a consortium managed by Ricardo Energy and Environment for the UK Department for Business, Energy and Industrial Strategy (BEIS) and the Department for Environment, Food and Rural Affairs (Defra). The NAEI is compiled on an annual basis according to internationally agreed methodologies (EMEP/EEA, 2019), encompassing sectors ranging from transport, industry, through to agriculture and domestic sources (Ricardo Energy and Environment, 2021). Here, we use the NAEI emissions from ~~2016~~ 2019, which is the most recent version publically available.~~as this was the most recent dataset~~

~~available when this work started and used in computationally time consuming model simulations (see Section 3.4). The most recent year now available is 2019. For comparison to top-down emissions estimates (see Section 3.3), using average $TCNO_2$ data centred on 2019, we extrapolate the NAEI 2016 emission values to 2019 levels for a more representative temporal comparison. The extrapolation was based on a simple linear trend (-3.9%/yr) for the NAEI UK NO_x total emissions between 2009 and 2018 (i.e. 10 years) and imposed on the NAEI 2016 gridded emissions.~~

2.2 Satellite Data

OMI and TROPOMI are both nadir-viewing instruments on-board the NASA Aura and ESA Sentinel 5 – Precursor (S5P) polar orbiting satellites, respectively, and have local overpass times of 13:30. TROPOMI measures in the ultraviolet-visible (UV-Vis, 270-500 nm), similar to OMI (Boersma et al., 2007), as well as near-infrared (NIR, 675-775 nm) and short-wave infrared (SWIR, 2305-2385 nm) spectral ranges (Veefkind et al., 2012). TROPOMI and OMI have nadir pixel sizes of 3.5 km × 5.5 km (in the UV-Vis, 7.0 km × 7.0 km for other spectral ranges) and 13 km × 24 km, respectively. The OMI (DOMINO version 2 product) and TROPOMI (TM5-MP-DOMINO version 1.2/3x – OFFLINE product) data were downloaded from the Tropospheric Emissions Monitoring Internet Service (TEMIS) for January 2005 to December 2015 and February 2018 to January 2020, respectively. Given the issues with large cloud cover in the UK, we use two years of TROPOMI $TCNO_2$ data to help increase the spatiotemporal sample size when deriving top-down emissions to evaluate the 2019 NAEI NO_x emissions. The OMI row anomaly first occurred in 2008 (Torres et al., 2018) and over time has progressively had a detrimental impact on retrieved $TCNO_2$. The study by Pope et al., (2018) successfully used the OMI record to look at long-term trends in UK $TCNO_2$. However, after 2015, while still retrieving robust signals over source regions, the row anomaly appears to be substantially artificially enhancing background $TCNO_2$. Therefore, as we consider regional trends in $TCNO_2$ in Section 3.2, we did not use OMI $TCNO_2$ after 2015. ~~We did not consider OMI $TCNO_2$ after 2015 as the row anomaly substantially degraded the quality of the data over the UK from this point.~~ The data has been processed using the methodology of Pope et al., (2018) to map the $TCNO_2$ data onto a high-resolution spatial grid (0.025° × 0.025°, ~2-3 km × ~2-3 km for TROPOMI, 0.05° × 0.05°, ~5 km × ~5 km for OMI). The TROPOMI data were quality controlled for a cloud radiance fraction <0.5, a quality control flag >~~50~~ 0.75 and where the $TCNO_2$ value was > -1.0×10^{-5} moles/m^2 (i.e. random values round 0.0 may be slightly negative or positive so we filter for $TCNO_2$ > -1.0×10^{-5} moles/m^2 otherwise a positive bias in average $TCNO_2$ is imposed). While TROPOMI provides the greatest spatial resolution of any satellite instrument to measure air pollutants, suitable to derive $TCNO_2$ emission estimates over UK city-scale sources, the retrieved $TCNO_2$ has been shown to have a low bias. Over north-western Europe, Verhoelst et al., (2021) found that TROPOMI underestimated $TCNO_2$ by approximately 20-30% when compared with surface $TCNO_2$ measurements, which is consistent with Chan et al., (2020) and Dimitropoulou et al., (2020). OMI data were processed for a geometric cloud fraction of <0.2, quality flag = 0 (which also flags pixels influenced by the row anomaly (Braak, 2010)) and $TCNO_2$ > -1.0×10^{-5} moles/m^2.

2.3 Simplified Mass Balance Approach

To derive top-down emissions of NO_2 we use the SMBA, which is based on downwind plumes of TROPOMI observed $TCNO_2$ from the target source where the observed total mass of NO_2 (i.e. the source-related enhancement of $TCNO_2$ above the background level) is assumed to be a product of the emission rate and the effective lifetime. Therefore, we can derive the emission rate based on **Equation 1**:

$$E = \frac{\sum_{i=0}^{N}(NO_2\ LD_i \times \Delta d)}{t \times e^{\frac{-t}{\tau}}} \qquad (1)$$

where E is the emission rate (moles/s), $NO_2\ LD$ is the NO_2 line density (moles/m), Δd is the grid box length (m), i is the grid box number between the source and background value, t is time (s) and $e^{\frac{-t}{\tau}}$ is the e-folding loss term with τ as the effective lifetime. N represents the number of satellite $TCNO_2$ grid boxes between the source and background level B. t is calculated as the distance between the source and B divided by the wind speed (ws). To derive the full NO_2 loading emitted from the source, ~~. The~~ the wind flow $NO_2\ LD$ ~~then~~ has the background $NO_2\ LD$ value subtracted from all points between the source and B and is then summed yielding the total NO_2 mass (moles).

The wind speed and direction at a particular source are determined from the European Centre for Medium-Range Weather Forecasts (ECMWF, 2021) ERA5 u- & v-wind component data. The wind data are sampled at 13:00 UTC (around 13:00 local solar time over the UK) to coincide with the TROPOMI overpass (i.e. 13:30 local solar time, LST) and averaged across boundary layer pressure levels (i.e. ~~1000~~ surface to ~~hPa and~~to ~~850~~ 900 hPa). In all cases, ws had to be greater than 2 m/s to avoid near stable meteorological conditions. Studies such as Beirle et al. (2011) and Verstraeten et al. (2018) averaged the wind speeds over the surface to 500 m layer. Beirle et al. (2011) suggested that the average winds across this altitude range yielded uncertainties over approximately 30%, but neither study provided definitive reasoning why 500 m was selected. In the UK, 500 m is approximately 950 hPa which sits comfortably within the boundary layer (approximately 1000 m or 880.0 to 910 hPa in **Figure 1a** based on ERA-5 data sampled at 13.00 LT and averaged for 2019). In this study, we argue that wind speeds throughout the boundary layer are likely to be important in controlling the spatial distribution of NO_2 downwind of sources. **Figure 1b** shows the zonally averaged latitude-pressure NO_2 profile from the Copernicus Atmosphere Monitoring Service (CAMS, 2021), sampled at 13.00 LT and averaged for 2019, over the UK. The bulk of the NO_2 loading is near the surface with NO_2 concentrations of 0.5 ppbv to >1.0 ppbv between the surface and 900 hPa. As shown by the white dashed lines, 60-70% of the surface to 500 hPa NO_2 loading exists between the surface and 900 hPa. The zonally averaged boundary layer pressure (red dashed line) also straddles the 900 hPa level. In **Figure 1c**, the wind speed profile for London sampled under westerly flow increases with altitude until between 925 hPa and 900 hPa. For each pressure level, London westerly days are defined based average u- and v-components between the surface and the respective pressure level. As shown by the blue text, the wind speed gradient with respect to pressure substantially decreases (i.e. from -0.0406 m/s/hPa between 950 hPa and 925 hPa to -0.0045 m/s/hPa between 925 hPa and 900 hPa) at 900 hPa. Therefore, this profile gradient and the information in **Figures 1a** & **b** suggest that 900 hPa is a suitable level to derive the boundary layer average wind speed and flow direction. The table (**panel d**) in **Figure 1** shows the sensitivity of the NO_x emission parameters to the pressure layer used. The derivation of emissions is discussed further in this section. The surface-850 hPa average and surface only winds show substantially different NO_x emission rates of 61.6

moles/s and 30.1 moles/s, respectively. However, the intermediate levels (900 hPa and 950 hPa) show less dramatic step changes with emission rates of 55.2 moles/s and 49.8 moles/s. Therefore, the surface-900 hPa layer is used to help derive NO_x emission rates in this study.

~~**Figure 1a** shows the difference between TROPOMI $TCNO_2$ sampled under westerly flow and the long-term average based on London u- and v-wind components.~~The *NO_2 LD* is the product of the source width, which is perpendicular to the wind flow, and the source-width-average $TCNO_2$ profile downwind from the source on a grid box by grid box basis as shown in **Equation 2**.

$$NO_2LD_{i=1,N} = \frac{\sum_{j=1}^{n} TCNO_{2i,j}}{n} \times w \times \alpha_i \qquad (2)$$

where *NO_2 LD* (moles of NO_2) is the NO_2 line density, *i* the grid box index downwind of the source starting at *i=1* going to *i=N* at background point *B*, *$TCNO_2$* is the tropospheric column NO_2 grid box value (moles/m^2) at point *i* and *j* is the grid box index for the number of grid boxes *n*, perpendicular to the downwind profile, which fit across the width of the source at grid box *i* downwind, *w* is the source width (m) (i.e. source width perpendicular to the downwind profile) of the NO_2 source and *α* is the grid box width (m) of the downwind grid box at point *i*. Though the source width is a subjective choice between the source edge locations, the same source width value is used when deriving the TROPOMI NO_x emissions and summing up the NAEI NO_x emissions over the source region. As the source emissions will be a function of the source width (i.e. larger at source centre and lower at source edge), the mean $TCNO_2$ downwind profile is representative of the source-average NO_2 emission. ~~The *NO_2 LD* is the product of the source width, which is perpendicular to the wind flow, and the source-width-average $TCNO_2$ profile downwind from the source. The $TCNO_2$ profile is the cross-section between the grid box the source centre is located in and the grid box where *B* is reached with units of moles/m^2. As there may be several downwind $TCNO_2$ profiles within the source width, these are averaged together to form an average downwind profile across the source width. As the source emissions will be a function of the source width (i.e. larger in source centre and lower at source edge), the mean $TCNO_2$ downwind profile is most representative of source-average NO_2 emission.~~

Figure 2a shows the difference between TROPOMI $TCNO_2$ sampled under westerly flow and the long-term average based on London u- and v-wind components, where there are clear downwind positive anomalies of >3.0 moles/m^2. Similarly in ~~As shown in~~ **Figure 2~~1~~b**, the downwind plume (e.g. westerly flow over London) has typically larger *NO_2 LD* values than the all-flow (i.e. all wind directions) *NO_2 LD*. The full NO_2 mass emitted from the source in the *NO_2 LD* is the summation of the wind-flow *NO_2 LD* from source up to point *B* minus the background value from all downwind pixels over this profile segment. ~~A~~ A reasonable estimate of when the wind-flow *NO_2 LD* reaches *B*, for more isolated NO_2 sources, is when it intersects with the all-flow *NO_2 LD* profile (i.e. returns to normal levels).~~A reasonable estimate of when the wind-flow *NO_2 LD* reaches *B* is when it intersects with the all-flow *NO_2 LD* profile (i.e. returns to normal levels).~~ However, when there are substantial upwind NO_2 sources, this can yield wind-flow *NO_2 LD* profiles which never intersect with the all-flow *NO_2 LD* profile within the domain (e.g. see Birmingham example in **Figure 3~~2~~a & b**). Therefore, to determine when *B* has been reached, a running t-test was applied to the wind-flow *NO_2 LD* profile to determine where turning points or levelling off occurred. As such a test can be sensitive to noise in the $TCNO_2$ data, a 10-pixel (0.5°) running average wind-flow *NO_2 LD* profile was calculated. The running

t-test was applied to this using two windows of the same size to identify step changes in the profile. The green line in **Figure 21~~1~~b** shows where the t-test p-value has become large and there is a turning point in the wind-flow *NO_2 LD* profile. Such a reduction in the wind-flow *NO_2 LD* profile gradient is suggestive of the plume reaching *B* as NO_2 levels have stabilised. However, in **Figure 21~~1~~b**, there are multiple locations potentially meeting this criteria. In reality, the turning points further downwind of London are sources from the Benelux region. The red dot represents the first instance, after the initial near-source wind-flow *NO_2 LD* peak, where the gradient in the running t-test p-value profile changes sign (i.e. positive to negative or vice versa)~~. The wind-flow *NO_2 LD* then has the background *NO_2 LD* value subtracted from all points between the source and *B* and is then summed yielding the total NO_2 mass (moles).~~. The loss term $e^{\frac{-t}{\tau}}$ is dependent upon τ and is determined by applying an e-folding distance fit between the near-source peak wind-flow *NO_2 LD* value and *B*, before dividing by *ws* to get τ. Here, a range of e-folding distances are tested in the loss term $e^{\frac{-t}{\tau}}$ to find the distance value which yields the lowest root mean square error (RMSE), and a large R^2 (Pearson correlation coefficient squared) value, between the e-folding distance fit (red line, **Figure 21~~c~~c**) and the wind-flow *NO_2 LD* (black line, **Figure ~~1c~~2c**). In the case of London, this yielded an e-folding distance of 148.0 km and τ of 4.5 hours (8.6 and 3.1 hours) based on the average *ws* = 9.1 m/s with an uncertainty range (± 4.3 m/s; i.e. ± 1-sigma standard deviation) of 4.8 m/s to 13.4 m/s (i.e. a slower/faster wind speed yields a longer/shorter lifetime).~~In the case of London, this yielded an e-folding distance of 150.0 km and τ of 3.8 hours (7.0 and 2.6 hours) based on *ws* = 9.9 m/s (± 4.6 m/s; i.e. ± 1-sigma standard deviation).~~ The effective lifetime derived here for London and other UK cities is typically consistent with values from other studies (e.g. Beirle et al., (2011) and Verstraeten et al. (2018)) for European cities (i.e. 1.0 –10.0 hours).

The top-down *E* is calculated from **Equation 1**, but this is an emissions flux of NO_2 moles/s which needs to be converted to NO_x for comparison with the bottom-up inventories. This is done by scaling the NO_2 emissions by 1.32 based on the NO:NO_2 concentration ratio (0.32) in urban environments at midday (Seinfeld and Pandis, 2006; Liu et al., 2016). Verstraeten et al., (2018) used modelled NO and NO_2 concentrations to derive a scaling more representative of the chemistry of the source. They estimate there is a 10% uncertainty (similar to Beirle et al., (2011)), but as the modelled NO_2:NO_x ratio is based on the input emissions, for which the satellite data is being used to evaluate, this process is rather circular and not independent. The final emission uncertainty estimates (**Figure 21~~1~~**) are derived by ± the satellite error (10^{-5} moles/m^2) before obtaining the *NO_2 LD* (Sat NO_x Emissions-1) and by using the uncertainties in τ when determining the loss term (Sat NO_x Emissions-2).

Here, the top-down NO_x emissions are derived by sampling $TCNO_2$ data under different wind directions in all seasons. Several studies, such as Beirle et al. (2011), have gone a step further and used $TCNO_2$ data to derive seasonal emissions. Unfortunately, here we are restricted to looking at annually derived emissions due to 1) the TROPOMI $TCNO_2$ record only started in February 2018, 2) the COVID-19 pandemic resulted in a dramatic reduction in UK (and global) NO_x emissions (Potts et al., 2021) meaning $TCNO_2$ data beyond February 2020 could not be used to derive top-down emissions under normal conditions and 3) the UK is subject to frequently cloudy conditions yielding a reduction in the number of observations from TROPOMI. The latter point predominantly influences TROPOMI retrievals in the winter-time. Therefore, even though we sample $TCNO_2$ data in all seasons, there is likely to be a tendency

towards summer-time $TCNO_2$ values, when $TCNO_2$ values tend to be lower (e.g. Pope et al., 2015), potentially leading to a low bias in the derived top-down NO_x emissions.

3. Results

3.1 NO_x Sources

Surface emissions and observed $TCNO_2$ represent different quantities and are influenced by different processes. However, the short NO_2 lifetime of a few hours (Schaub et al., 2007; Pope et al., 2015) means there is a sharp gradient between sources and the background levels. Therefore, we can use the satellite $TCNO_2$ observations to provide some constraint on the spatial distribution of the NO_x emissions. In **Figure 43**, spatial maps over south-eastern (**Figure 43a & c**) and northern England (**Figure 43b & d**) show evidence of co-located $TCNO_2$ and NO_x emission hot spots, especially over many of the UK cities shown by circles. Here, both data sets have been mapped onto the spatial resolution of 0.025° × 0.025°. In South East England, $TCNO_2$ and NO_x emissions peak over London at over 14.0×10^{-5} moles/m^2 and approximately >2.0 μg/m^2/s, respectively. A secondary peak is also observed over western London for both quantities at similar levels. There are further co-located hotspots over Southampton ($TCNO_2$ ~$8.0\text{-}9.0\times10^{-5}$ moles/m^2, NO_x >2.0 μg/m^2/s), Portsmouth ($TCNO_2$ ~$6.0\text{-}7.0\times10^{-5}$ moles/m^2, NO_x ~1.0-1.5 μg/m^2/s), Brighton ($TCNO_2$ ~$5.0\text{-}6.0\times10^{-5}$ moles/m^2, NO_x ~0.5-0.8 μg/m^2/s), Oxford ($TCNO_2$ ~$7.0\text{-}7.5\times10^{-5}$ moles/m^2, NO_x ~0.7-1.0 μg/m^2/s) and Chelmsford ($TCNO_2$ ~$8.5\text{-}9.5\times10^{-5}$ moles/m^2, NO_x ~0.5 μg/m^2/s). In northern England and the Midlands, peak $TCNO_2$ and NO_x emissions are located over Manchester ($TCNO_2$ ~$10.0\text{-}11.0\times10^{-5}$ moles/m^2, NO_x ~1.0-1.5 μg/m^2/s), Birmingham ($TCNO_2$ ~$8.0\text{-}9.0\times10^{-5}$ moles/m^2, NO_x ~1.0-1.5 μg/m^2/s), Leeds ($TCNO_2$ ~$8.0\text{-}9.0\times10^{-5}$ moles/m^2, NO_x ~1.0-1.5 μg/m^2/s) and Liverpool ($TCNO_2$ ~$7.0\text{-}8.0\times10^{-5}$ moles/m^2, NO_x ~0.5-1.0 μg/m^2/s).

To quantify the spatial relationship between the $TCNO_2$ and NO_x emissions over source regions, the corresponding pixels of both data sets were sub-sampled for each UK city (79 in total), normalised by the sample mean and correlated against each other (red circles, **Figure 43e**), which yielded a correlation $R_{city1x1}$ = 0.358 (i.e. city1×1 represents 1 grid box × 1 grid box or 0.025° × 0.025° around where the city centre is located). However, as atmospheric NO_2 is subject to chemical reactions and meteorological processes (e.g. transport), the signal around source regions is more diluted and the peak $TCNO_2$ not necessarily centred on the source. To allow for that, the spatial resolution of the quantities over each source was degraded, averaging over 3×3 (**Figure 43f**), 5×5 (**Figure 34g**) and 7×7 (**Figure 43h**) grid cells and the correlation recalculated (e.g. city3x3 represents 3 grid box × 3 grid box or 0.075° × 0.075° around where the city centre is located). This resulted in correlations of $R_{city3x3}$ = 0.513, $R_{city5x5}$ = 0.6258 and $R_{city7x7}$ = 0.52. The correlation for full domain (i.e. the UK) was R_{all} = 0.2014. As expected, the correlation for all grid pixels (e.g. including pixels over the sea) is weak where long-range transport of NO_2 can yield spatial variability in background regions with corresponding zero emission pixels. The $R_{city1x1}$, $R_{city3x3}$, $R_{city5x5}$ and $R_{city7x7}$ correlations were all larger. The largest city-scale correlation was for the $R_{city5x5}$ values where the spatial variability has been smoothed and is representative of the more diffuse pattern of $TCNO_2$. However, the $R_{city7x7}$ (0.175° × 0.175° or ~15-20 km × 15-20 km) correlation is lower than the $R_{city5x5}$ value suggesting that this scale is larger than most UK city sizes. Overall, for all R values, except for R_{all}, there are statistically significant positive correlations at the 90% confidence level (CL) or

above (>95% CL for $R_{city3x3}$, $R_{city5x5}$ and $R_{city7x7}$). Therefore, the city-scale emission-satellite correlations provide confidence in the spatial distribution of the NAEI NO_x emissions based on the observed satellite $TCNO_2$.

3.2 Satellite NO_2 and Emission NO_x Trends

To evaluate the temporal evolution of the NAEI emissions, we use the long-term satellite record of $TCNO_2$ from OMI between 2005 and 2015. Annual total UK emissions of NO_x (~~treated~~ expressed as NO_2 here) from the NAEI start in 1970 and continue to present day (typically with a lag of approximately two years). Annual spatial maps of the NAEI also exist over the same time period. However, while there is a consistent methodology for the UK total estimates, the mapping methodology updates between years (NAEI, 2017). Therefore, instead of performing trends on the maps, we focus on trends in the UK NO_x emission totals. For OMI, we have taken a similar broad scale approach focussing on averaged $TCNO_2$ across England (defined as 3°W-2°E, 50-54°N). We focus on England as the majority of large UK sources with reasonable spatiotemporal coverage are located here and have clearly defined trends over source regions. Pope et al., (2018) showed significantly (at the 95% CL) decreasing trends over London, Birmingham, Manchester and the Yorkshire power stations of between 1.5% and 2.3% per year. OMI measurements can be subject to large uncertainties and variability, so this analysis also investigates trends in a range of OMI $TCNO_2$ percentiles over time. To estimate the annual absolute England total NAEI NO_x emissions, we summed the emissions data for England (same geographical definition as for OMI above) from the ~~2016~~ 2019 NAEI NO_x emissions map and imposed the UK total NO_x trend on it. Here, we use a simple linear fit which yields an annual decrease in the UK total NO_x emission of 4.4%. The relative rate of change is the same for the England total NO_x emissions, but the absolute values are lower than the UK total NO_x emissions (**Figure 5~~4~~, top panel**).

Over the 2005-2015 period, the England average OMI $TCNO_2$ trends in the 10^{th}, 25^{th}, 50^{th}, 75^{th} and 90^{th} percentiles are -0.18 $\times10^{-5}$ moles/m^2/yr (-3.3%/yr), -0.20 $\times10^{-5}$ moles/m^2/yr (-2.7%/yr), -0.21 $\times10^{-5}$ moles/m^2/yr (-2.2%/yr), -0.17 $\times10^{-5}$ moles/m^2/yr (-1.3%/yr) and -0.07 $\times10^{-5}$ moles/m^2/yr (-0.4%/yr), respectively (**Figure 4~~5~~**). All of the satellite trends are significant at the 95% CL except for the 90^{th} percentile. The UK and England total NO_x emission trends between 2005 and 2015 are -76~~49~~.3~~7~~ kt/yr and -45~~30~~.5~~1~~ kt/yr (both -4.4%/yr). The OMI $TCNO_2$ trends range between -3.2% and -0.4% depending on the data percentile used to generate the average England $TCNO_2$ annual time series. We also calculated annual trends in UK and England (same definition as above) surface NO_2 observations (**Figure 5~~4~~**, bottom panel) from AURN (AURN, 2021). Here, we used urban background, suburban and rural sites. For the 10^{th}, 25^{th}, 50^{th}, 75^{th} and 90^{th} percentiles, UK (England) trends are -0.26 (-0.27) µg/m^3/yr, -0.40 (-0.52) µg/m^3/yr, -0.73 (-0.77) µg/m^3/yr, -0.95 (-0.95) µg/m^3/yr and -1.19 (-1.09) µg/m^3/yr. This corresponds to -3.77 (-3.03) %/yr, -3.07 (-3.24) %/yr, -3.03 (-2.86) %/yr, -2.49 (-2.31) %/yr and -2.29 (-1.98) %/yr. Therefore, the NAEI NO_x emissions trend is of similar magnitude and direction to that of the observations. The differences are most likely explained by the non-linear conversion of emissions to atmospheric concentrations (i.e. complex meteorology and chemistry). The likely drivers for decreases in UK NO_x emissions and NO_2 concentrations include a shift to cleaner energy sources (e.g. National Emissions Ceilings Regulations 2018, DEFRA. (2018b)), regulations on industrial and power generation emissions (Environmental Permitting Regulations 2016 (UK Government, 2016)) and tighter emissions

for vehicles (e.g. Euro 6 emissions standards). Overall, these results provide confidence in the use of the satellite data as a tool to evaluate bottom-up emissions trends.

3.3 Top-Down NO_x Emissions

The top-down NO_x emission rate for London under westerly flow (**Figure 21**) is 558.27 moles/s (375.57, 749.8 moles/s, based on Sat NO_x Emissions-1 uncertainties), while the NAEI flux is 302.97 moles/s. Here, the NAEI has a low bias with the top-down estimate and sits outside the uncertainty range. The top-down emissions are based on 2 years, so the flux should be representative of an annual emission rate, corresponding to the NAEI reporting. In the case of Birmingham (**Figure 32a**), under easterly flow, there is a visible plume (i.e. positive differences of 2.0-3.0×10^{-5} moles/m^2) superimposed on a background enhancement (0.5-1.0×10^{-5} moles/m^2). As a result, the wind-flow *NO_2 LD* is always larger than the all-flow *NO_2 LD* and never reaches the background level (i.e. zero differences in **Figure 32a**) within the domain for which the TROPOMI $TCNO_2$ data has been processed for (e.g. there are positive differences in between the source, Birmingham, and the west of the domain, 8°W). Therefore, the running t-test methodology is used to determine when the wind-flow *NO_2 LD* reaches a steady background state *B*, as shown in **Figure 32b**. Overall, the NAEI (124.89 moles/s) underestimates the top-down emissions for Birmingham under easterly flow (29.07.3 (187.78, 369.92) moles/s).

Our methodology was applied to 10 city sources where sources had suitable downwind $TCNO_2$ enhancements to derive *NO_2 LDs* and top-down emissions (**Figure 6**). A suitable downwind $TCNO_2$ enhancement was subjectively identified when a clear $TCNO_2$ enhancement (i.e. positive anomalies) under a specific wind flow/direction occurred and a realistic lifetime (i.e. in the range of the literature – e.g. Verstraeten et al. (2018)) could be derived from the downwind $TCNO_2$ profile of the target source. ~~Our methodology was applied to 12 city sources where sources had suitable downwind $TCNO_2$ enhancements to derive *NO_2 LDs* and top-down emissions (**Figure 5**).~~ These are shown in **Table 1**. Where top-down emissions could be derived for sources over several wind directions, they were averaged together. The $TCNO_2$ response to mesoscale and synoptic weather systems (i.e. large scale flow) can be seasonally influenced (e.g. Pope et al., 2015) with some wind directions occurring more frequently in certain seasons. Therefore, top-down NO_x emission estimates derived from several wind directions for a particular source, though sampled throughout all months, can vary depending on the seasonal influence on the observed $TCNO_2$ for which the wind direction more frequently occurs in. The top-down emissions derived here suggest that the NAEI bottom-up emissions for the largest sources such as London, Manchester and Birmingham are underestimated. The top-down emissions for London, Manchester and Birmingham are 47.99.2 (312.78, 654.90) moles/s, 20.519.7 (132.20, 287.13) moles/s and 221.10, (143.65, 298.86) moles/s with corresponding NAEI emissions of 302.9 7 moles, 10.60 moles/s and 124.97 moles/s, respectively. ~~Note for Birmingham though, the NAEI emissions value sits within the top-down estimate uncertainty range.~~

For the smaller sources (e.g. Edinburgh, Bristol and ~~Norwich~~Cardiff), the comparisons are in better agreement with the NAEI and are located within the top-down emission ranges. However, for Newcastle the NAEI emissions (34.10 moles/s) are substantially larger than the top-down estimate (1.97 (0.8, 2.96) moles/s). In contrast, for Leeds (3.70 moles/s), Norwich (1.0 moles/s and Belfast (1.6 moles) ~~(3.5 moles/s) and Glasgow (5.5 moles)~~, the NAEI

substantially underestimates the top-down emissions of 5.750 (3.76, 7.65) moles/s, 2.4 (1.3, 3.4) moles/s and 93.4 (25.18, 4.813.8) moles/s, respectively. For several of the top-down For the estimates under 10.0 moles/s, the NO_2 effective lifetime, we find it ranges between 2.91.75 and 37.9 .5 hours hours, which is . These lifetimes are at the lower range of expected consistent with values in the literature values (e.g. Schaub et al., 2007; Pope et al., 2015), which in turn may yield positively skewed top-down estimates (e.g. Leeds and Glasgow). For all cities in **Figure 56** there is a strong correlation (0.99) between the NAEI and top-down emission sources investigated here, but the NAEI has a bias of -4.18 moles/s (-37.4%) low bias of 2.95 moles/s (28.3%) on average, dominated by the larger sources (i.e. London, Manchester and Birmingham). These metrics were calculated in linear space.

3.4 Comparison of GEOS-Chem and Observation NO_2

As the input emissions for GEOS-Chem come from the NAEI (2016 NAEI emissions scaled to 2019), any inconsistencies between simulated and observed NO_2 potentially indicates discrepancies in the underlying emissions. Such emission discrepancies, inferred by the model, and consistent with top-down – NAEI NO_x emission differences would help act as a verification of the top-down emissions. **Figure 6** represents comparisons between GEOS-Chem and TROPOMI $TCNO_2$ between January and June 2019. In the case of London, there is a clear model underestimation of over 3.0×10^{-5} moles/m^2 and the green polygon-outlined region shows where the absolute bias lies outside the satellite uncertainty range. A similar substantial negative bias (-2.0 to -1.0×10^{-5} moles/m^2) is found over Manchester. This suggests that the model, driven by the NAEI, substantially underestimates TROPOMI and that therefore the input emissions may be too low. For Birmingham, the GEOS-Chem-TROPOMI $TCNO_2$ biases are smaller peaking at 0.25×10^{-5} moles/m^2.

However, over some regions comparisons with TROPOMI show model positive biases (~$1.0-2.0\times10^{-5}$ moles/m^2). Investigation of January only shows that modelled $TCNO_2$ is substantially larger than TROPOMI across most of the central and north-eastern England. This is potentially suggestive of issues in the model's representation of the winter-time boundary layer where too much NO_2 is trapped (not shown here). When January is removed from the 2019 average, a larger negative GEOS-Chem-TROPOMI $TCNO_2$ bias is produced over Birmingham (-0.5×10^{-5} moles/m^2). Therefore, this again suggests that the NAEI NO_x emissions may be too low when compared to the top-down estimate here.

We also compared GEOS-Chem with surface AURN NO_2 data from sites across the UK and sub-sampled to 13:00 LST each day to match the TROPOMI overpass and model output times, between January and June 2019. On average, there is a UK negative model AURN bias of -9.96 µg/m^3. A substantial proportion of the bias will be the comparison of area-weighted model surface NO_2 against point measurement NO_2 observations. Here, the model horizontal resolution is too coarse to adequately represent smaller NO_2 sources (i.e. roads and point industry sources), while the AURN point measurements will be heavily influenced by higher resolution sources (Savage et al., 2013). AURN NO_2 measurements also use the chemiluminescence technique with molybdenum converters, which may overestimate true NO_2 concentrations and thus further compound the model negative bias (Savage et al., 2013 and references therein). When we compare the model against AURN for London, Birmingham and Manchester (averaging AURN sites within the city domains listed in **Table 1**) we find model biases of -15.3 µg/m^3, -8.1 µg/m^3 and 19.0 µg/m^3, respectively. Unfortunately, all the

~~other cities in **Figure 5** are limited to one AURN site at most. Therefore, one site is unlikely to be representative of city scale NO_2 level and thus our analysis is limited to these three large cities. Overall, the model AURN NO_2 negative biases at London and Manchester are larger than the UK average negative bias, and support our hypothesis that the NAEI NO_x emissions are underestimated for London and Manchester. The model negative bias at Birmingham is of similar size to the UK average and thus suggestive that the NAEI NO_x emissions over Birmingham are more reasonable.~~

4. Conclusions

We have evaluated relationships between satellite observations (TROPOspheric Monitoring Instrument, TROPOMI) of tropospheric column nitrogen dioxide ($TCNO_2$) and the UK National Atmospheric Emissions Inventory (NAEI) for nitrogen oxides (NO_x = NO + NO_2). Although they are different quantities, the short NO_2 lifetime means that our comparison can serve as a useful and important tool to evaluate bottom-up emissions. Here, spatial comparison of the TROPOMI $TCNO_2$ with the NAEI highlights consistency over the source regions with co-located peak values in the respective data sets. Correlation analysis of $TCNO_2$ and NO_x emissions over the UK cities indicates moderate spatial agreement with R ranging between 0.4 and 0.6 (significant at the >90% confidence level). Analysis of long-term satellite records of $TCNO_2$ (from the Ozone Monitoring Instrument (OMI), 2005-2015) show comparable negative trends with the NAEI NO_x emissions with rates of -2.2%/yr and -4.4%/yr, respectively. Though the relative NAEI trend is larger than OMI, meteorological conditions and photochemistry will control the atmospheric response to a change in NO_x emissions, as seen by OMI. It is also possible that the NAEI overestimates the decreasing NO_x emissions trend.

We have also used TROPOMI data to derive top-down city-scale estimates of UK NO_x emissions. While it can still be challenging to derive emissions from ~~moderately~~ city scale ~~sized~~ sources (e.g.~~e.g.~~ frequent cloud cover in the UK~~cities such as Bristol and Cardiff~~), we estimate top-down emissions fluxes (using satellite data between February 2018 and January 2020) for several ~~larger sources~~ cities. Most of the city sources show reasonable agreement, but for larger sources like ~~(i.e.~~ London~~,~~ ~~and~~ Manchester and Birmingham ~~)~~, the top-down ~~and find~~ emission values are substantially larger than those in the NAEI for 2019. ~~(i.e. 2016 emissions scaled to 2019). When these NAEI emissions are used to drive the GEOS-Chem atmospheric chemistry model, we find substantial negative biases between the model and satellite/surface observations for London and Manchester. Therefore, this provides further evidence that the NAEI emissions for London and Manchester may be underestimated. Other sources, with lower emission rates (e.g. below 10.0 moles/s), tend to be in reasonable agreement between both datasets (i.e. NAEI emission rate is within the top-down emission uncertainty range).~~

Overall, as far as we are aware, this study represents the first robust attempt to use satellite observations of $TCNO_2$ to evaluate and constrain the official UK bottom-up NAEI. We find spatial and temporal agreement between the two quantities, but find evidence that the NAEI NO_x emissions for larger sources (e.g. London) may be too low (i.e. by >25%) sitting outside the top-down emission uncertainty ranges (i.e. based on the satellite retrieval errors). To fully

understand the discrepancies and the drivers of these NO_x emissions differences, further investigation is required.

Data Availability

TROPOMI and OMI tropospheric column NO_2 data comes from the Tropospheric Emissions Monitoring Internet Service (TEMIS, https://www.temis.nl/airpollution/no2.php). The bottom-up NO_x emissions come from the National Atmospheric Emissions Inventory (https://naei.beis.gov.uk/data/data-selector?view=air-pollutants) and the point and area sources can be obtained from https://naei.beis.gov.uk/data/map-uk-das?pollutant_id=6&emiss_maps_submit=naei-20210325121854. The specific UK total NO_x emissions came from https://naei.beis.gov.uk/data/data-selector-results?q=142818. Meteorological wind, temperature and boundary layer height data came from ECMWF (https://cds.climate.copernicus.eu/cdsapp#!/dataset/reanalysis-era5-pressure-levels?tab=overview). ~~Meteorological wind data came from ECMWF (https://cds.climate.copernicus.eu/cdsapp#!/dataset/reanalysis-era5-pressure-levels?tab=overviewhttps://cds.climate.copernicus.eu/cdsapp#!/dataset/reanalysis-era5-pressure-levels?tab=overview).~~ CAMS NO_2 data was retrieved form https://ads.atmosphere.copernicus.eu/cdsapp#!/dataset/cams-global-reanalysis-eac4?tab=form.The AURN data was obtained from https://uk-air.defra.gov.uk/networks/network-info?view=aurn.

Author contribution

RJP undertook the research looking at the spatial maps and long-term trends. RJP, RK, CW and AMG worked on the satellite top-down city-scale NO_x emission estimates. ~~EAM provided the GEOS-Chem simulations.~~ RJP prepared the manuscript with contributions from all co-authors.

Competing interests

The authors declare that they have no conflict of interest.

Acknowledgements

This work was funded by the Department for Environment, Food and Rural Affairs Affairs through the "Applying Earth Observation (EO) to Reduce Uncertainties in Emission Inventories" project and by the UK Natural Environment Research Council (NERC) by providing funding for the National Centre for Earth Observation (NCEO, award reference NE/R016518/1).

References

AURN. Automated Urban and Rural Network [Online]. Available: https://uk-air.defra.gov.uk/networks/network-info?view=aurn (accessed 30th March 2021), 2021.

Beirle, S., Boersma, B.F., Platt, U., Lawrence, M.G. and Wagner, T.: Megacity emissions and lifetimes of nitrogen oxides probed from space, *Science*, 333, 1737, doi:10.1126/science.1207824, 2011.

Boersma, K.F., Eskes, H.J., Veefkind, J.P., Brinksma, E.J., van der A, R.J., Sneep, M., van den Oord, G.H.J., Levelt, P.F., Stammes, P., Gleason, J.F. and Bucsela, E.J.: Near-real time

retrieval of tropospheric NO_2 from OMI, *Atmospheric Chemistry and Physics*, 7, 2103–2118, doi:10.5194/acp-7-2103-2007, 2007.

Braak R. 2010. Row Anomaly Flagging Rules Lookup Table, KNMI Technical Document TN-OMIE-KNMI-950, *KNMI*, Netherlands.

CAMS. CAMS global reanalysis (EAC4). Available: https://ads.atmosphere.copernicus.eu/cdsapp#!/dataset/cams-global-reanalysis-eac4?tab=form (accessed 29th November 2021), 2021.

Chan, K. L., Wiegner, M., van Geffen, J., De Smedt, I., Alberti, C., Cheng, Z., Ye, S. and Wenig, M.: MAX-DOAS measurements of tropospheric NO_2 and HCHO in Munich and the comparison to OMI and TROPOMI satellite observations, *Atmospheric Measurement Techniques*, 13, 4499–4520, doi: 10.5194/amt-13-4499-2020, 2020.

DEFRA. Air Pollution in the UK 2017 [Online]. Available: https://uk-air.defra.gov.uk/assets/documents/annualreport/air_pollution_uk_2017_issue_1.pdf (last accessed 30th March 2021), 2018a.

DEFRA. UK Informative Inventory Report (1990 to 2016) [Online]. Available: https://uk-air.defra.gov.uk/library/reports?report_id=956 (last accessed 30th March 2021), 2018b.

DEFRA. Air Pollution in the UK 2019 [Online]. Available: https://uk-air.defra.gov.uk/library/annualreport/viewonline?year=2019_issue_1#report_pdf (accessed 30th March 2021), 2020.

Dibbens, C. and Clemens, T.: Place of work and residential exposure to ambient air pollution and birth outcomes in Scotland, using geographically fine pollution climate mapping estimates, *Environmental Research*, 140, 535-541, doi:10.1016/j.envres.2015.05.010, (2015).

Dimitropoulou, E., Hendrick, F., Pinardi, G., Friedrich, M. M., Merlaud, A., Tack, F., De Longeville, H., Fayt, C., Hermans, C., Laffineur, Q., Fierens, F. and Van Roozendael, M.: Validation of TROPOMI tropospheric NO_2 columns using dual-scan multi-axis differential optical absorption spectroscopy (MAX-DOAS) measurements in Uccle, Brussels, *Atmospheric Measurement Techniques*, 13, 5165–5191, doi: 10.5194/amt-13-5165-2020, 2020.

ECMWF. ERA5 hourly data on pressure levels from 1979 to present. Available at: https://cds.climate.copernicus.eu/cdsapp#!/dataset/reanalysis-era5-pressure-levels?tab=overview (accessed 29th November 2021), 2021.

EEA. Air quality in Europe — 2018 report [Online]. Available: https://www.eea.europa.eu/publications/air-quality-in-europe-2018 (accessed 30th March 2021), 2018.

EMEP/EAA. EMEP/EEA air pollutant emission inventory guidebook 2019, EEA Report No 13/2019, ISSN 1977-8449. Available: https://www.eea.europa.eu/publications/emep-eea-guidebook-2019 (accessed 2nd July 2021), 2019.

EMEP. EMEP – Convention on Long-range Transboundary Air Pollution. Available: https://www.emep.int/ (accessed 12th July 2021), 2021.

Liu, F., Beirle, S., Zhang, Q., Dörner, S., He, K. and Wagner T.: NOx lifetimes and emissions of cities and power plants in polluted background estimated by satellite observations, *Atmospheric Chemistry and Physics,* 16, 5283-5298, doi:10.5194/acp-16-5283-2016, 2016.

Martin, R.V., Jacob, D.J., Chance, K., Kurosu, T.P., Palmer, P.I. and Evans, M.J.: Global inventory of nitrogen oxide emissions constrained by space-based observations of NO_2 columns, *Journal of Geophysical Research,* 108, 4537, doi:10.1029/2003JD003453, 2003.

Miyazaki, K., Eskes, H., Sudo, K., Boersma, K.F., Bowman, K. and Kanaya, Y.: Decadal changes in global surface NO_x emissions from multi-consistent satellite data assimilation, *Atmospheric Chemistry and Physics,* 17, 807-837, doi:10.5194/acp-17-807-2017, 2016.

NAEI. UK Emission Mapping Methodology. – 2015 [Online]. Available: https://uk-air.defra.gov.uk/assets/documents/reports/cat07/1710261436_Methodology_for_NAEI_2017.pdf (accessed 30th March 2021), 2017.

NAEI. UK-NAEI – National Atmospheric Emissions Inventory [Online]. Available: https://naei.beis.gov.uk/ (accessed 30th March 2021), 2021.

Pena-Angulo, D., Reig-Gracia, F., Dominguez-Castro, F., Revuelto, J., Aguilar, E., van der Schrier, G. and Vicente-Serrano, S. M.: ECTACI: European Climatology and Trends Atlas of Climate Indices (1979-2017), *Journal of Geophysical Research: Atmospheres*, 125, e2020JD032798, doi: 10.1029/2020JD032798, 2020.

Pope, R.J., Savage, N.H., Chipperfield, M.P., Ordonez, C. and Neal, L.S.: The influence of synoptic weather regimes on UK air quality: Regional model studies of tropospheric column NO_2, *Atmospheric Chemistry and Physics,* 15, 11201-11215, doi:10.5194/acp-15-11201-2015, 2015.

Pope, R.J., Arnold, S.R., Chipperfield, M.P., Latter, B.G., Siddans, R. and Kerridge, B.J.: Widespread changes in UK air quality observed from space, *Atmospheric Science Letters,* 19, e817, doi: 10.1002/asl.817, 2018.

Potts, D.A., Marais, E.A., Boesch, H., Pope, R.J., Lee, J., Drysdale, W., Chipperfield, M.P., Kerridge, B. and Siddans, R.: Diagnosing air quality changes in the UK during the COVID-19 lockdown using TROPOMI and GEOS-Chem, *Environmental Research Letters,* 16, 054031, doi:10.1088/1748-9326/abde5d, 2021.

Ricardo Energy and Environment. UK Informative Inventory Report (1990 to 2019). Available: https://uk-air.defra.gov.uk/assets/documents/reports/cat09/2103151107_GB_IIR_2021_FINAL.pdf (accessed 2nd July 2021), 2021.

Royal College of Physicians. Every breath we take: the lifelong impact of air pollution [Online]. Available: https://www.rcplondon.ac.uk/projects/outputs/every-breath-we-take-lifelong-impact-air-pollution (accessed 30th March 2021), 2016.

Savage, N.H., Agnew, P., Davis, L.S., Ordóñez, C., Thorpe, R., Johnson, C.E., O'Connor, F.M. and Dalvi, M.: Air quality modelling using the Met Office Unified Model (AQUM OS24-26): model description and initial evaluation, *Geoscientific Model Development,* 6, 353–372, doi:10.5194/gmd-6-353-2013, 2013.

Schaub, D., Brunner, D., Boersma, K.F., Keller, J., Folini, D., Buchmann, B., Berresheim, H. and Staehelin, J.: SCIAMACHY tropospheric NO_2 over Switzerland: estimates of NOx lifetime

and impacts of the complex alpine topography on the retrieval, *Atmospheric Chemistry and Physics,* 7, 5971-5987, doi:10.5194/acp-7-5971-2007, 2007.

Seinfeld, J. and Pandis, S.: Atmospheric Chemistry and Physics: From Air Pollution to Climate Change - Second Edition, John Wiley and Sons Inc, New Jersey, USA, 2006.

Torres, O., Bhartia, P. K., Jethva, H. and Ahn, C.: Impact of the ozone monitoring instrument row anomaly on the long-term record of aerosol products, *Atmospheric Measurement Techniques*, 11, 2701-2715, doi:10.5194/amt-11-2701-2018, 2018.

Tsagatakis, I., Richardson, J., Evangelides, C., Pizzolato, M., Pearson, B., Passant, N., Pommier, M. and Otto, A.: UK Spatial Emissions Methodology: A report of the National Atmospheric Emission Inventory 2019. Available at: https://uk-air.defra.gov.uk/assets/documents/reports/cat09/2107291052_UK_Spatial_Emissions_Methodology_for_NAEI_2019_v1.pdf (accessed 29th November 2021), 2021.

UK Government. The Environmental Permitting (England and Wales) Regulations 2016. Available: https://www.legislation.gov.uk/uksi/2016/1154/contents/made (last accessed 2nd July 2021), 2016.

Veefkind, J.P., Aben, I., McMullan, K., Forster, H., de Vries, J., Otter, G., Claas, J., Eskes, H.J., de Haan, F., Kleipool, Q., van Weele, M., Hasekamp, O., Hoogeveen, R., Landgraf, J., Snel, R., Tol, P., Ingmann, P., Voors, R., Kruizinga, B., Vink, R., Visser, H. and Levelt, P.F.: TROPOMI on the ESA Sentinel-5 Precursor: A GMES mission for global observations of atmospheric composition for climate, air quality and ozone layer applications, *Remote Sensing of Environment,* 120, 70-83, doi:10.1016/j.rse.2011.09.027, 2012.

Verhoelst, T., Compernolle, S., Pinardi, G., Lambert, J. C., Eskes, H., Eichmann, K. U., et al.: Ground-based validation of the Copernicus Sentinel-5P TROPOMI NO2 measurements with the NDACC ZSL-DOAS, MAX-DOAS and Pandonia global networks, *Atmospheric Measurement Techniques*, 14, 481–510, doi: 10.5194/amt-14-481-2021, 2021.

Verstraeten, W.W., Boersma, K.F., Douros, J., Williams, J.E., Eskes, H., Liu, F., Beirle, S. and Delcloo, A.: Top-down NO_x emissions of European cities based on the downwind plume of modelled and space-borne tropospheric NO_2 column, *Sensors,* 18 (9), 2893, doi:10.3390/s18092893, 2018.

WHO. Ambient (outdoor) air pollution [Online]. Available: https://www.who.int/news-room/fact-sheets/detail/ambient-(outdoor)-air-quality-and-health (last accessed 30th March 2021), 2018.

Wu, H., Reis, S., Lin, C. and Heal, M.R.: Effect of monitoring network design on land use regression models for estimating residential NO_2 concentration, *Atmospheric Environment,* 149, 24-33, doi:10.1016/j.atmosenv.2016.11.014, 2017.

Figures

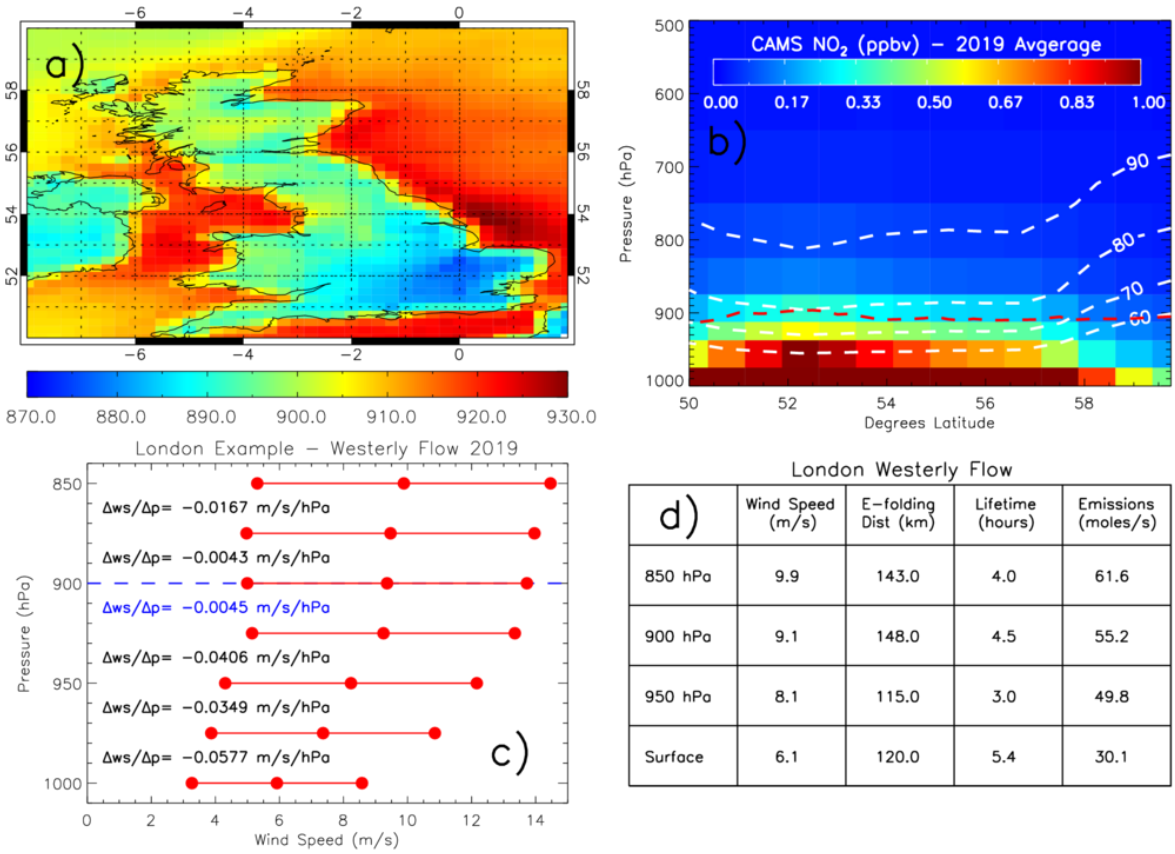

London Westerly Flow

d)	Wind Speed (m/s)	E-folding Dist (km)	Lifetime (hours)	Emissions (moles/s)
850 hPa	9.9	143.0	4.0	61.6
900 hPa	9.1	148.0	4.5	55.2
950 hPa	8.1	115.0	3.0	49.8
Surface	6.1	120.0	5.4	30.1

Figure 1: *a) ERA-5 UK boundary layer pressure (hPa) sampled at 13.00 LT (to coincide with the TROPOMI overpass time) and averaged for 2019. b) CAMS reanalysis zonal (8.0°W-2.0°E) average latitude-pressure NO_2 (ppbv) cross-section over the UK between the surface and 500 hPa. White dashed lines represent the percentage of the surface-500 hPa NO_2 loading between the surface and the respective pressure levels. The red dashed line represents the zonal average boundary layer pressure (hPa). c) Average (surface to pressure level) wind speed (m/s), ± the standard deviation, profile over London under westerly flow (determined from the ERA-5 u-wind and v-wind components at each pressure level). Δws/Δp is the wind speed gradient between pressure levels. The blue text indicates the first small step change in the gradient indicative of reduced flow turbulence and a suitable surface-altitude range to average the winds speeds over. d) The table shows the impact to the NO_x emission parameters when using different altitudes over which to average the wind speeds.*

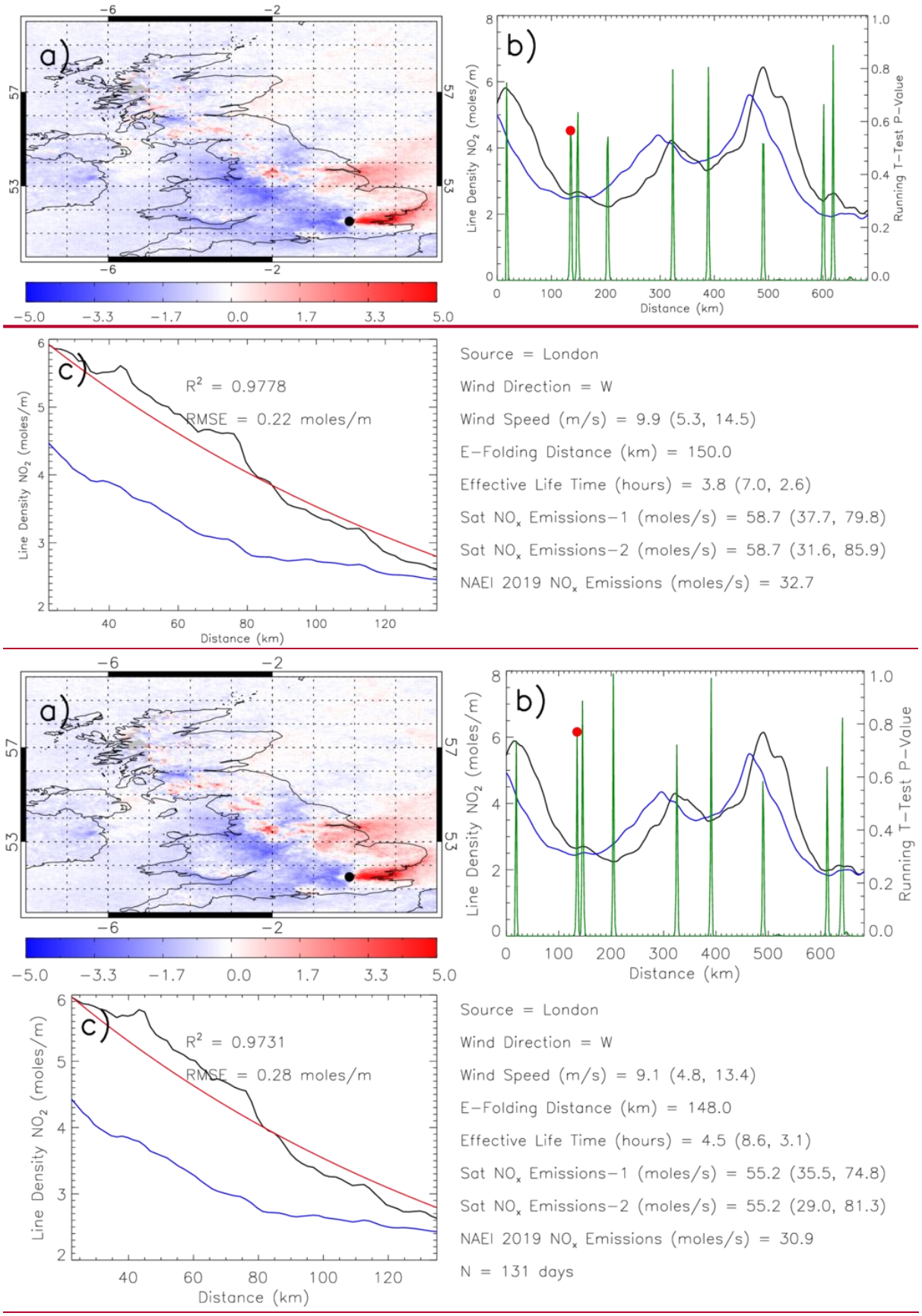

Figure 2~~1~~: *(a) TROPOMI TCNO$_2$ (10^{-5} moles/m^2) sub-sampled under westerly flow (defined over London, black dot) minus the long-term average (February 2018 to January 2020). (b)*

Downwind NO_2 LD from London (black = westerly flow, blue = all-flow average) with the corresponding running t-test p-value (green line). The red dot represents the location of background level determined by the turning point in the running t-test p-value time series. (c) The westerly flow and all-flow NO_2 LD between peak westerly flow NO_2 LD and the background value. The red line represents the e-folding distance fit with the corresponding R^2 and root mean square error (RMSE) between the westerly flow NO_2 LD and fit profile. N represents the number of days classified under westerly flow over London.

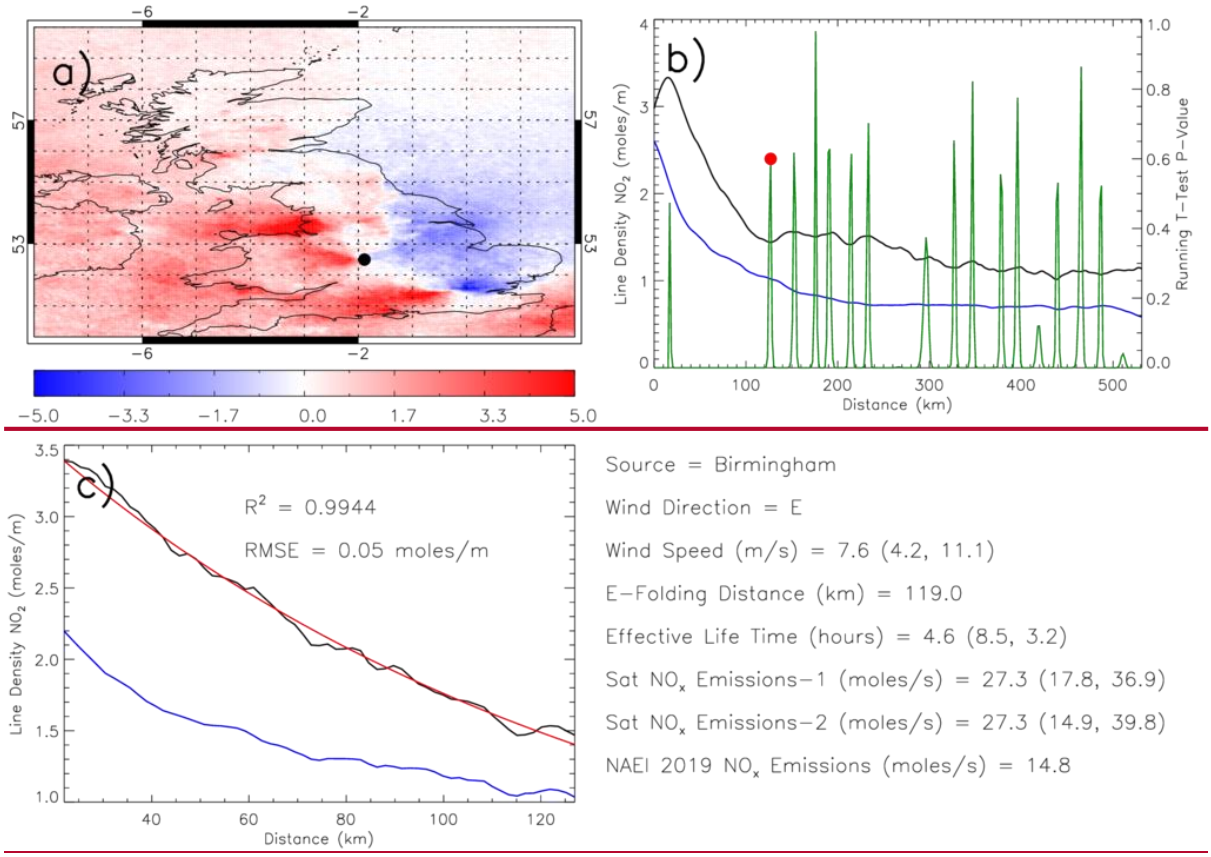

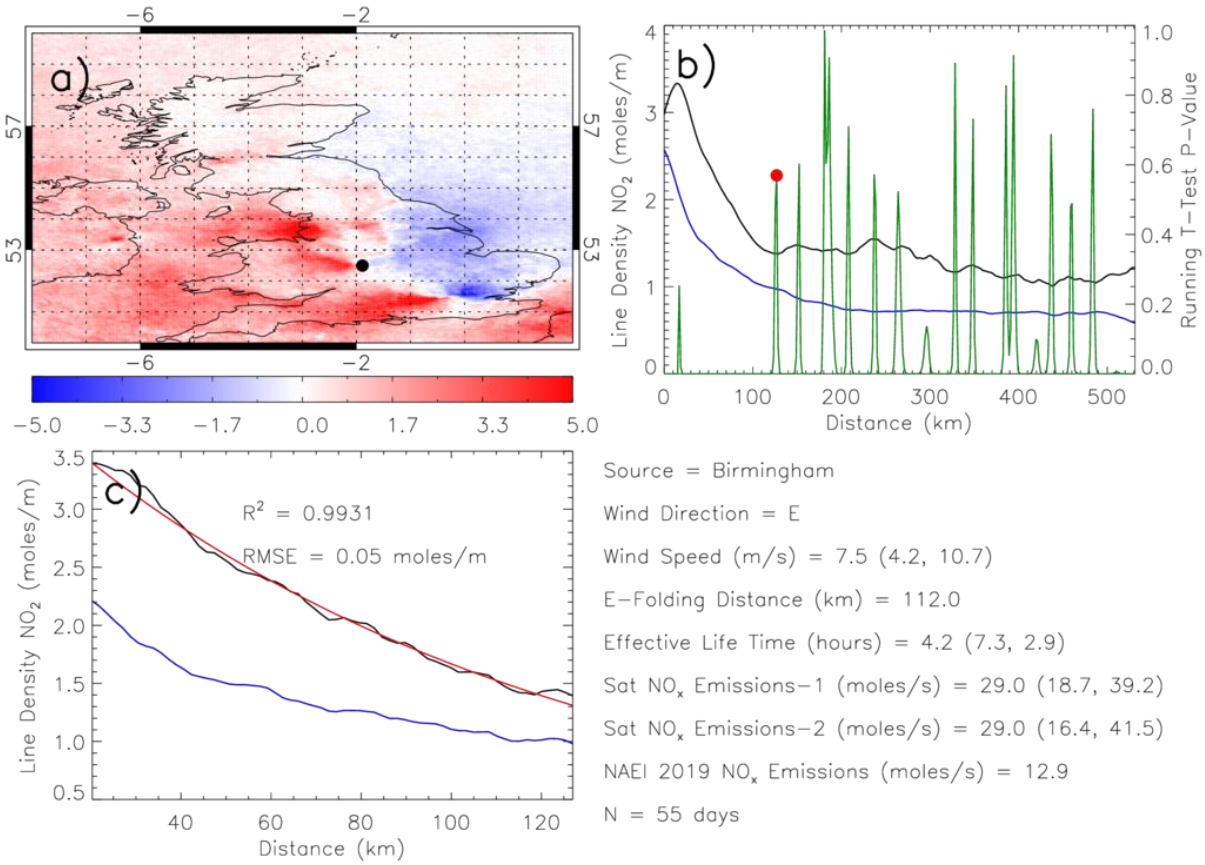

Figure ~~32~~: *(a) TROPOMI TCNO₂ (10^{-5} moles/m²) sub-sampled under easterly flow (defined over Birmingham, black dot) minus the long-term average (February 2018 to January 2020). (b) Downwind NO₂ LD from Birmingham (black = easterly flow, blue = all-flow average) with the corresponding running t-test p-value (green line). The red dot represents the location of background level determined by the turning point in the running t-test p-value time series. (c) The easterly flow and all-flow NO₂ LD between peak easterly flow NO₂ LD and the background value. The red line represents the e-folding distance fit with the corresponding R^2 and root mean square error (RMSE) between the easterly flow NO₂ LD and fit profiles. N represents the number of days classified under easterly flow over Birmingham.*

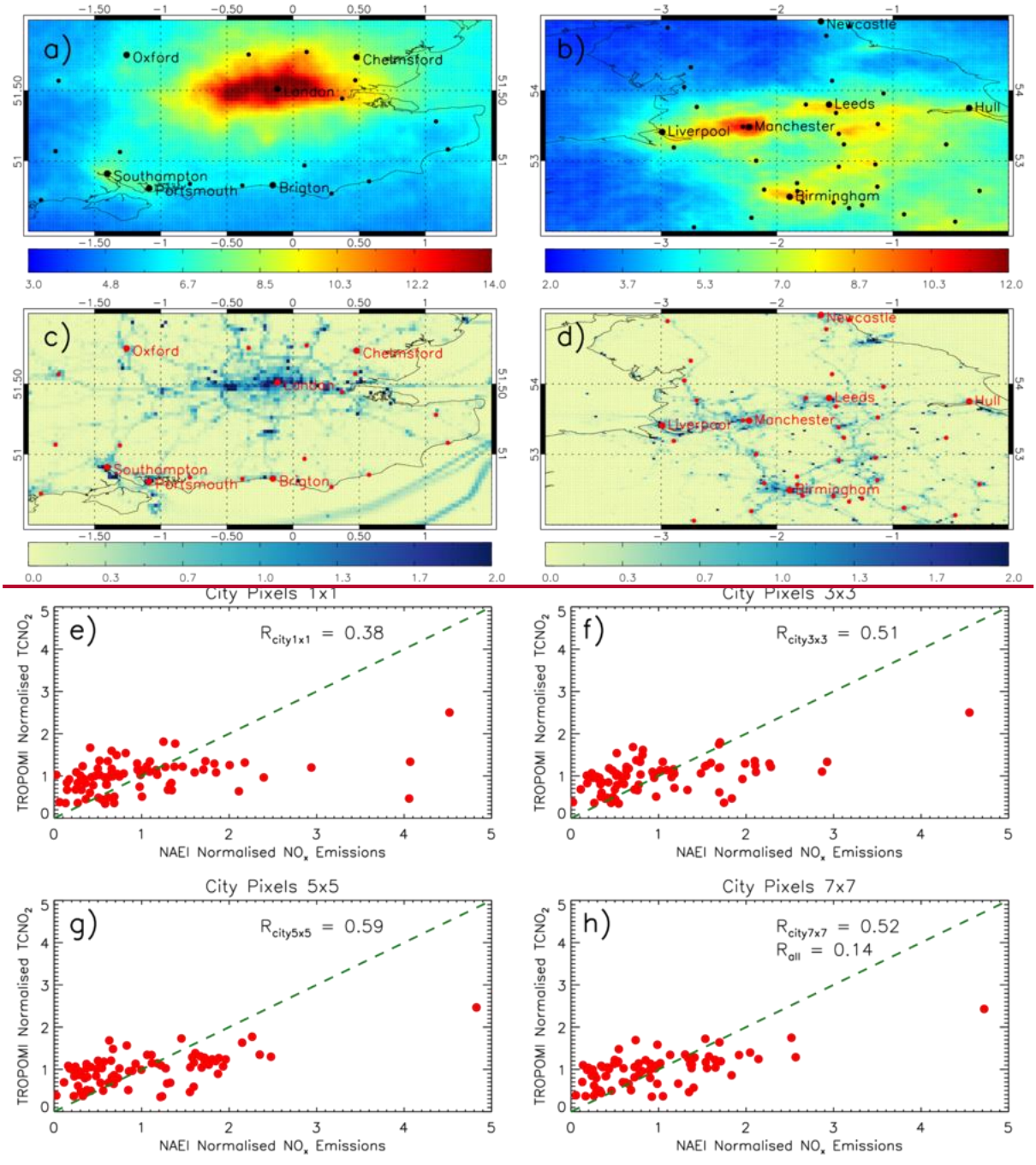
a)
Oxford
Chelmsford
London
Southampton
Portsmouth
Brigton
b)
Newcastle
Leeds
Hull
Liverpool
Manchester
Birmingham
c)
d)
City Pixels 1x1
City Pixels 3x3
City Pixels 5x5
City Pixels 7x7
e)
f)
g)
h)
$R_{city1x1}$ = 0.38
$R_{city3x3}$ = 0.51
$R_{city5x5}$ = 0.59
$R_{city7x7}$ = 0.52
R_{all} = 0.14
TROPOMI Normalised $TCNO_2$
NAEI Normalised NO_x Emissions

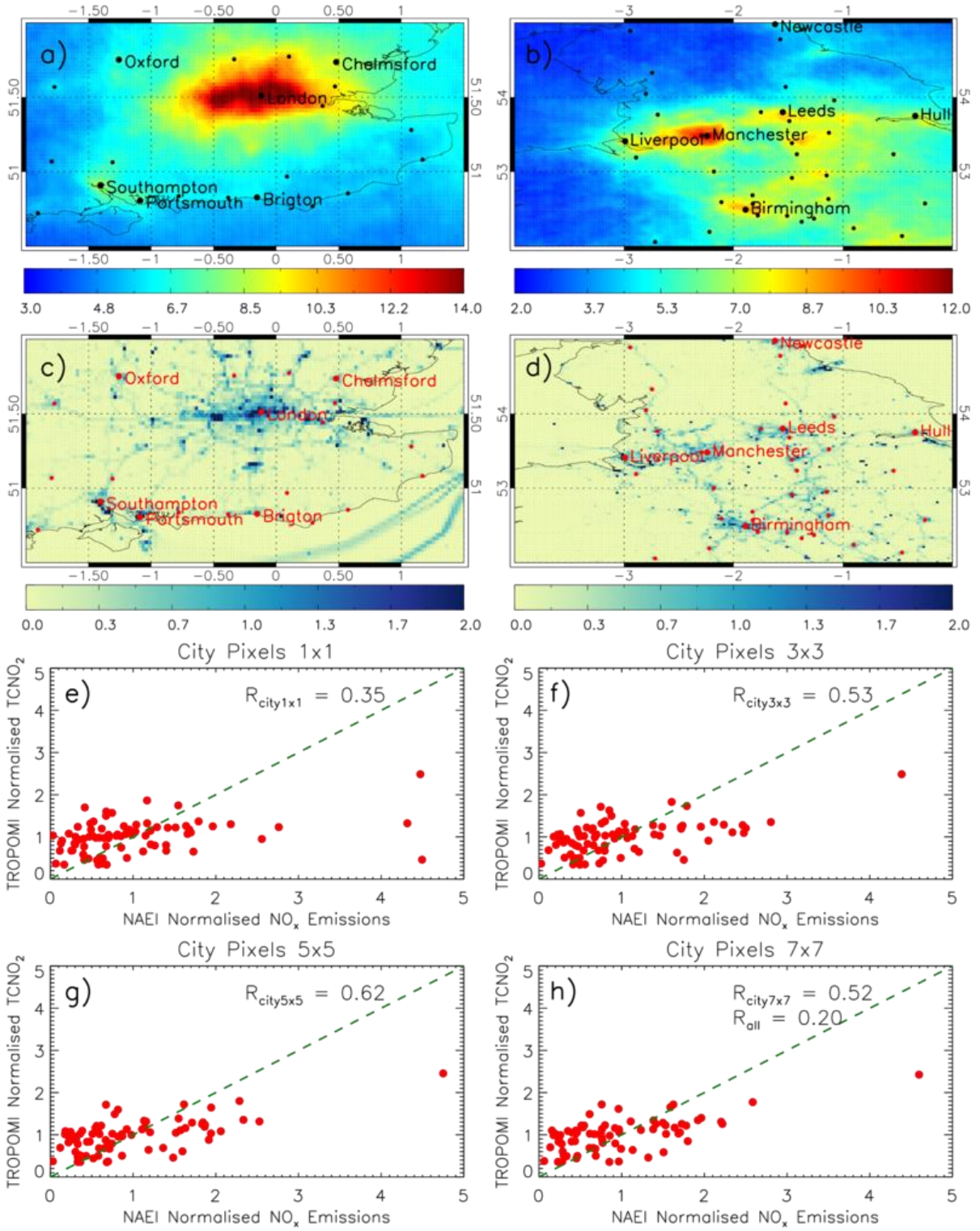

Figure 4~~3~~: *TROPOMI $TCNO_2$ ($\times 10^{-5}$ moles/m^2) average for February 2018 to January 2020 across (a) south-eastern and (b) northern England. Black circles represent city locations. NAEI NO_x emissions (µg/m^2/s) for 201~~6~~9 across (c) south-eastern and (d) northern England. Red circles represent city locations. Panels (e)-(h) represent the correlation of normalised $TCNO_2$ and NO_x emissions for UK cities. The green dashed line is the 1:1 line. Each source is normalised by the average of all the sources. The four panels also represent city means using*

varying pixel ranges around the source (i.e. 1×1, 3×3, 5×5 and 7×7 grid pixels). The correlations between the city-scale normalised NO_x emissions and $TCNO_2$ are shown (R).

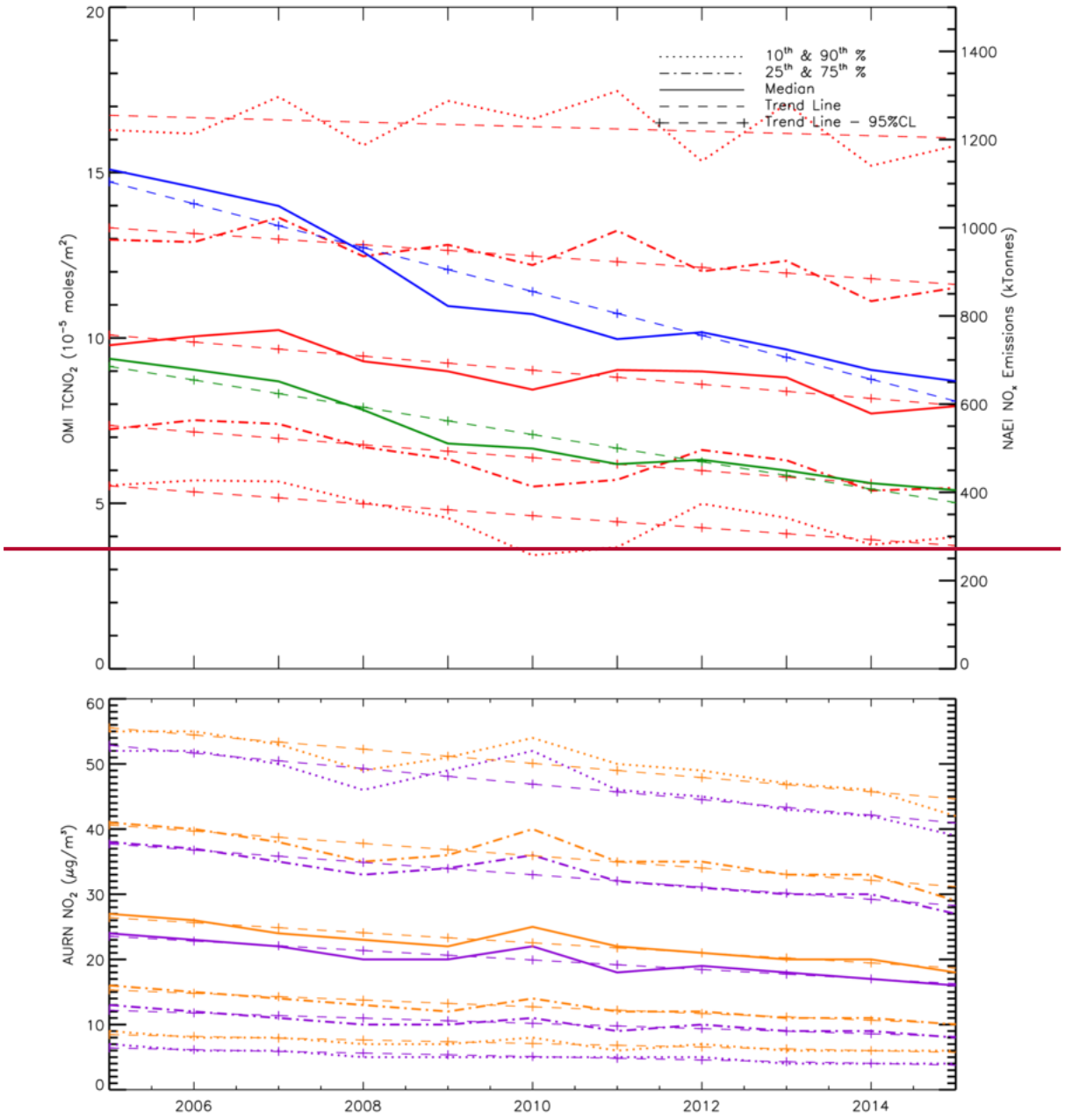
10th & 90th %
25th & 75th %
Median
Trend Line
Trend Line – 95%CL
OMI TCNO2 (10-5 moles/m2)
NAEI NOx Emissions (kTonnes)
AURN NO2 (μg/m3)
2006
2008
2010
2012
2014

780

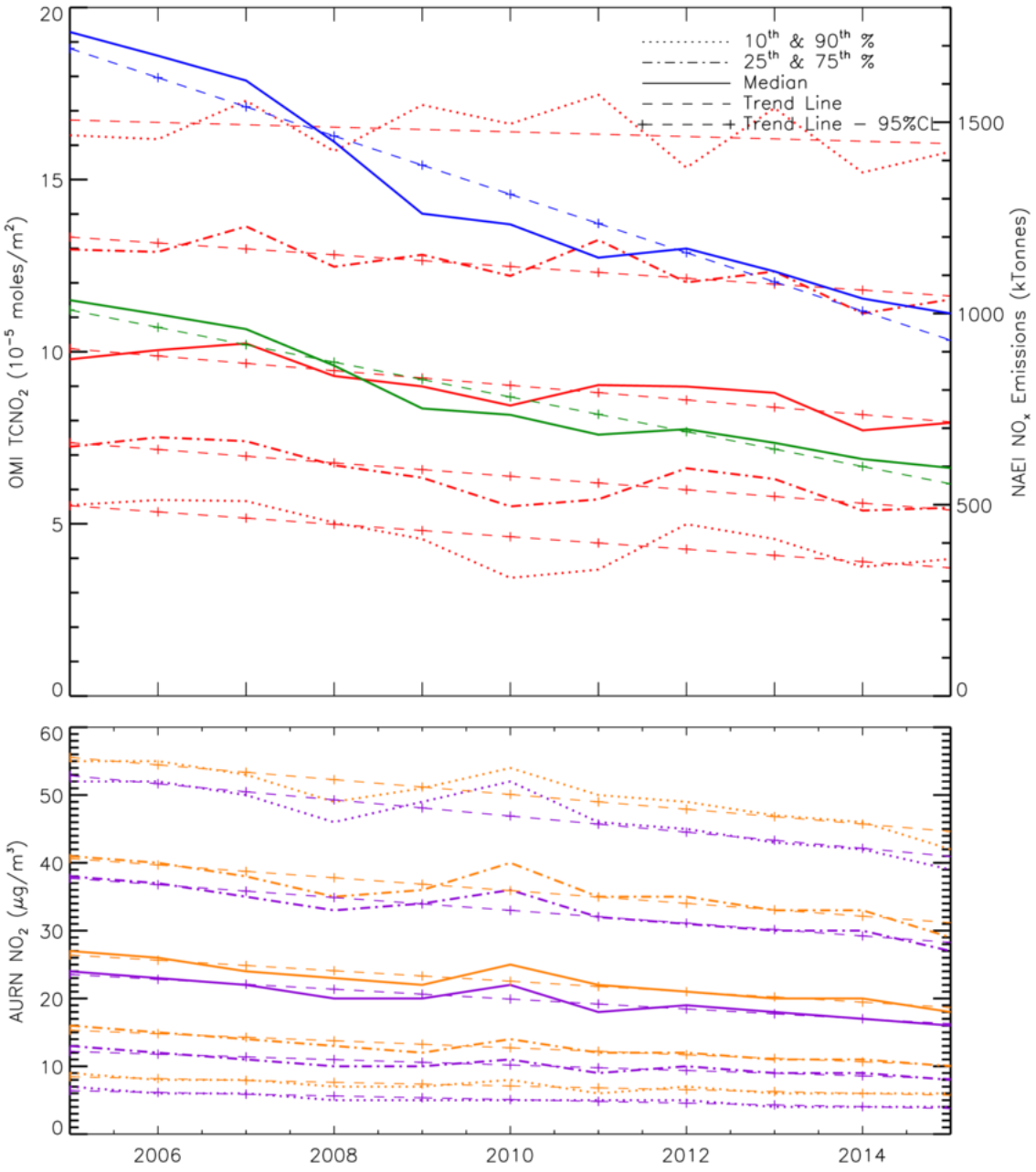

Figure 54: *The top panel shows time series (2005 to 2015) in OMI $TCNO_2$ ($\times 10^{-5}$ moles/m^2) and NAEI NO_x emission totals (kt or Gg). OMI median, 10th & 90th and 25th & 75th percentiles are represented by solid, dotted and dot-dashed lines, respectively. NAEI NO_x emission totals for the UK and England are represented by the blue and green solid lines. Here, the OMI $TCNO_2$ has been averaged over England (defined as 3°W-2°E, 50-54°N) and while the UK NO_x emission totals are directly reported by the NAEI, the England NO_x emission totals have been summed over the emissions maps for the same England definition used for OMI (see Section 3.2 for more information).* In the bottom panel, *AURN surface NO_2 (μg/m^3) ~~trends~~ times series are shown for the UK (purple) and England (orange).* Trends lines are shown by dashed and dash-crossed lines for insignificant and significant trends (at the 95% confidence level).

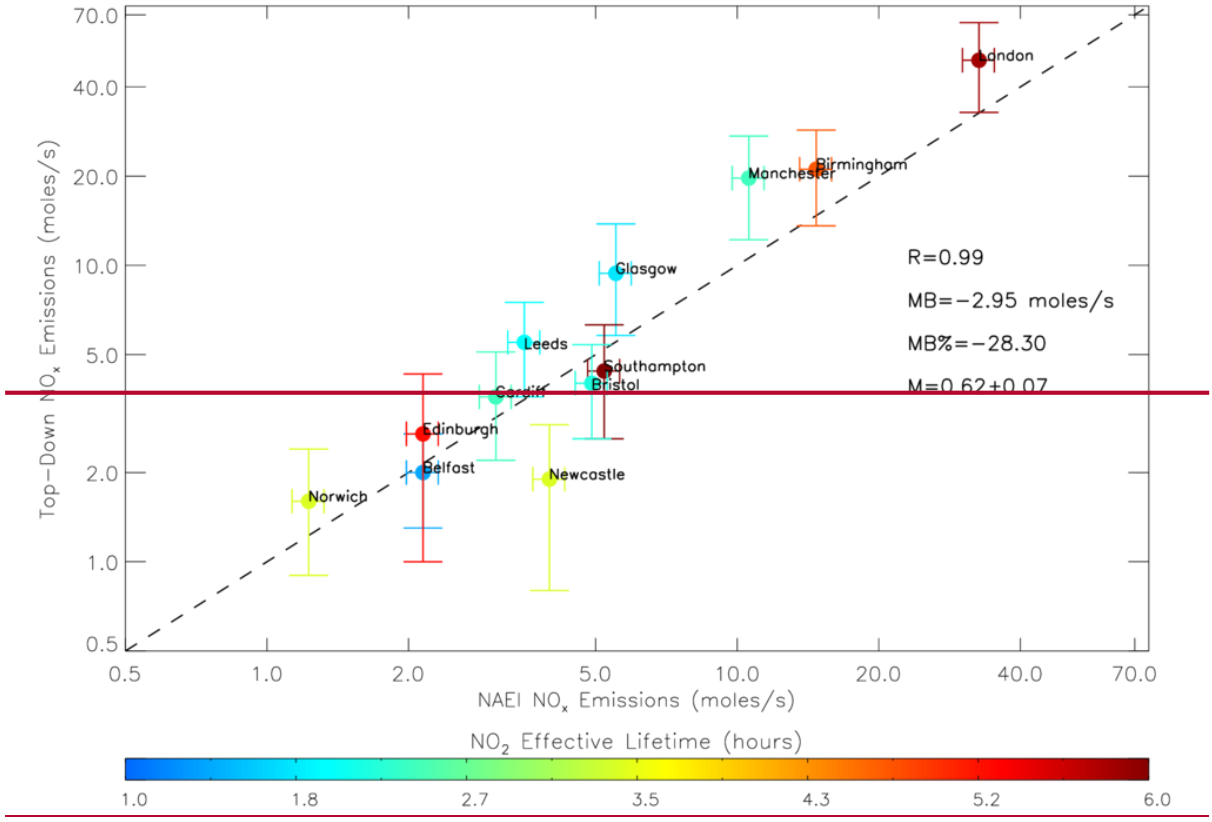

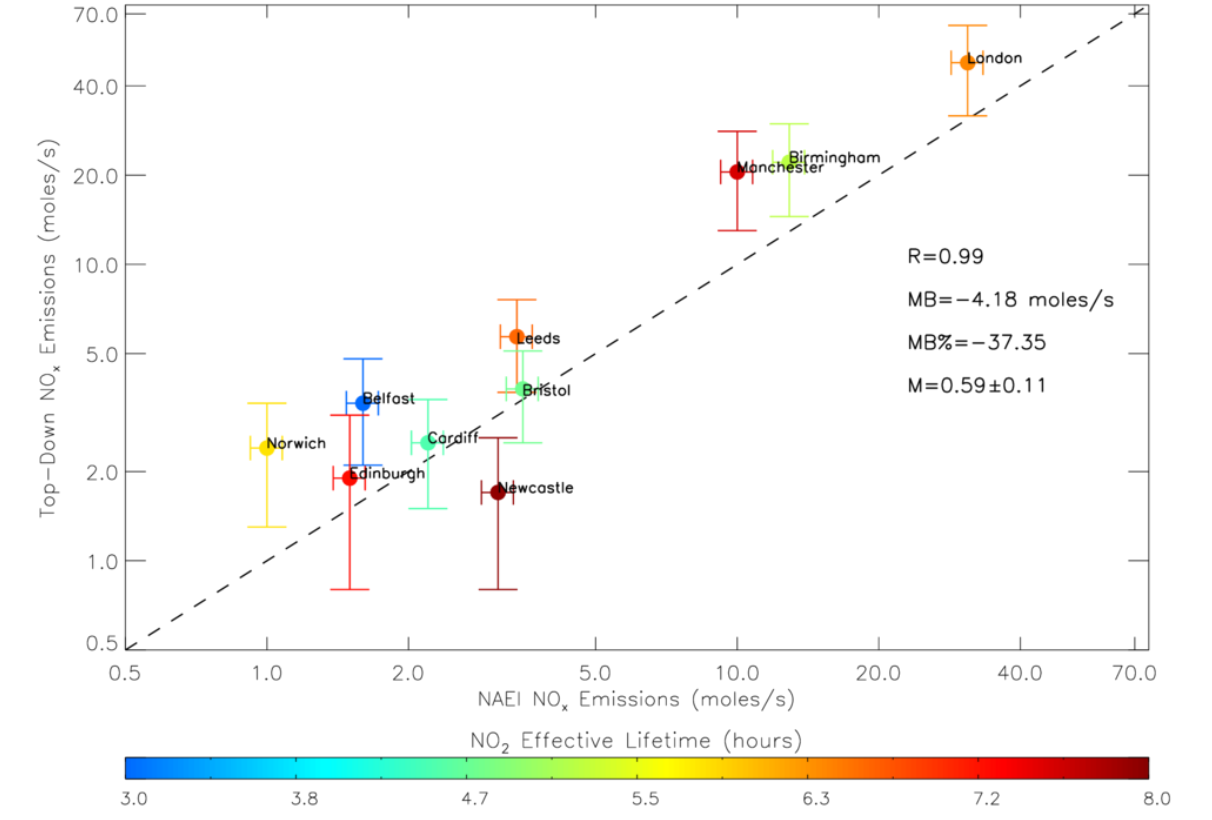

Figure ~~6~~5: *NAEI and top-down (TROPOMI) NO_x emissions (moles/s) for 1~~2~~0 UK cities coloured by the NO_2 effective lifetime (hours). Where there is more than one top-down estimate for a city from multiple wind directions, the corresponding emission rates and lifetimes have been*

averaged together. The correlation (R), mean bias (MB, moles/s), percentage mean bias (MB%) and linear fit (M) are also shown. *NAEI uncertainty is ±7.8% (DEFRA, 2018b) and the top-down uncertainty range is based on satellite errors (i.e. Sat Emissions-1, see text). The black dashed line represents the 1:1 relationship and both axes are on log scales.*

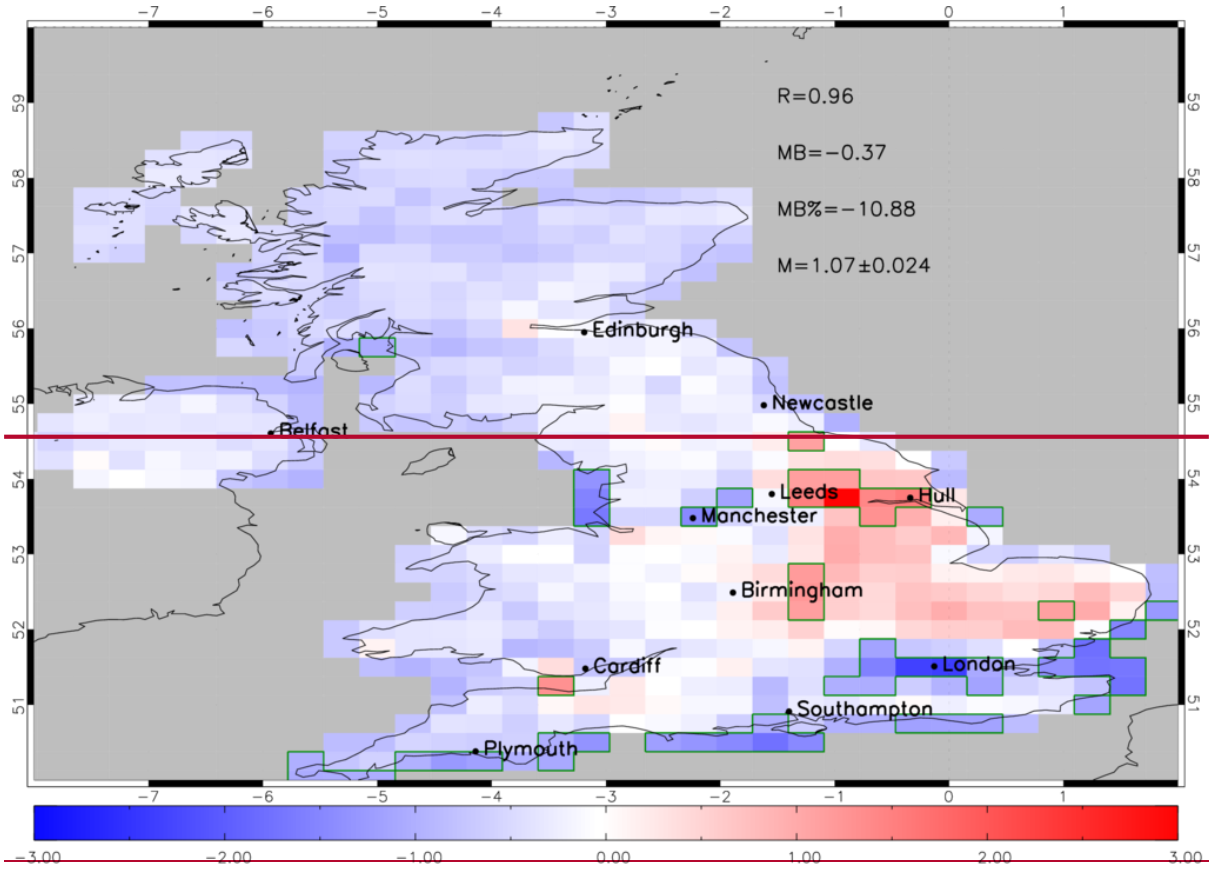

~~**Figure 6:** *GEOS-Chem minus TROPOMI mean $TCNO_2$ (10^{-5} moles/m^2) for January to June 2019. The green polygon outlined regions represent where the absolute model-satellite bias is greater than the satellite error (i.e. |mod-sat| > sat error) and the absolute bias (|mod-sat|) is greater than $1.0×10^{-5}$ moles/m^2 (i.e. where biases are the same order of magnitude as the mean $TCNO_2$ state). The domain correlation (R), mean bias (MB), percentage mean bias (MB%) and linear fit (M) are shown.*~~

Table 1: *List of top-down NO_x (moles/s) emission estimates for UK city sources under different wind directions. Sat NOx Emissions-1 represents the emission flux estimated using the TROPOMI NO_2 ± the retrieval uncertainty, while Sat NOx Emissions-2 is based on the lifetime derived from the wind speed data ± 1.0 sigma standard deviation.*

Source Name	London	London	London	Birmingham
Longitude	-0.13	-0.13	-0.13	-1.89
Latitude	51.51	51.51	51.51	52.50
Lon Edge - West	-0.52	-0.52	-0.52	-2.18
Lon Edge - East	0.28	0.28	0.28	-1.72
Lat Edge - South	51.32	51.32	51.32	52.35
Lat Edge - North	51.69	51.69	51.69	52.66
Wind Speed Average (m/s)	9.10	7.00	7.50	7.50
Wind Speed Standard Deviation (m/s)	4.30	3.20	3.10	3.20
Wind Direction	W	N	E	E
E-Folding Distance (km)	148.00	189.00	195.00	112.00
Life Time (hr)	4.50	7.50	7.20	4.20
Life Time- Lower Wind (hr)	8.60	13.80	12.40	7.30
Life Time- Upper Wind (hr)	3.10	5.20	5.10	2.90
Satellite Emission Rate (moles/s)	55.20	55.90	32.50	29.00
Sat NOx Emissions-1 - Lower (moles/s)	35.50	37.40	22.10	18.70
Sat NOx Emissions-1 - Upper (moles/s)	74.80	74.30	42.80	39.20
Sat NOx Emissions-2 - Lower (moles/s)	29.00	30.50	18.80	16.40
Sat NOx Emissions-2 - Upper (moles/s)	81.30	81.20	46.10	41.50
NAEI Emission Rate (moles/s)	30.90	30.90	30.90	12.90

Source Name	Birmingham	Birmingham	Newcastle	Manchester
Longitude	-1.89	-1.89	-1.62	-2.25
Latitude	52.50	52.50	54.98	53.50
Lon Edge - West	-2.18	-2.18	-1.73	-2.47
Lon Edge - East	-1.72	-1.72	-1.40	-2.01
Lat Edge - South	52.35	52.35	54.92	53.37
Lat Edge - North	52.66	52.66	55.02	53.60
Wind Speed Average (m/s)	5.80	9.10	10.50	5.60
Wind Speed Standard Deviation (m/s)	2.60	4.70	4.30	2.50
Wind Direction	N	S	W	N
E-Folding Distance (km)	184.00	91.00	297.00	152.00
Life Time (hr)	8.70	2.80	7.90	7.50
Life Time- Lower Wind (hr)	15.80	5.80	13.60	13.60
Life Time- Upper Wind (hr)	6.00	1.80	5.60	5.20
Satellite Emission Rate (moles/s)	12.20	25.20	1.70	20.5
Sat NOx Emissions-1 - Lower (moles/s)	8.10	16.70	0.80	13.00

Sat NOx Emissions-1 - Upper (moles/s)	16.40	33.70	2.60	28.10
Sat NOx Emissions-2 - Lower (moles/s)	6.80	12.20	1.00	11.30
Sat NOx Emissions-2 - Upper (moles/s)	17.70	38.20	2.40	29.80
NAEI Emission Rate (moles/s)	12.90	12.90	3.10	10.00

834

Source Name	Belfast	Edinburgh	Norwich	Cardiff
Longitude	-5.93	-3.19	1.29	-3.18
Latitude	54.61	55.96	52.63	51.49
Lon Edge - West	-6.00	-3.32	1.20	-3.36
Lon Edge - East	-5.84	-3.10	1.38	-3.10
Lat Edge - South	54.55	55.89	52.60	51.45
Lat Edge - North	54.70	55.98	52.69	51.55
Wind Speed Average (m/s)	8.30	10.10	10.30	5.30
Wind Speed Standard Deviation (m/s)	4.10	4.20	4.8	2.50
Wind Direction	E	W	W	N
E-Folding Distance (km)	87.00	262.00	214.00	86.00
Life Time (hr)	2.90	7.20	5.80	4.50
Life Time- Lower Wind (hr)	5.80	12.20	11.00	8.60
Life Time- Upper Wind (hr)	1.90	5.10	3.90	3.00
Satellite Emission Rate (moles/s)	3.40	1.90	2.40	2.50
Sat NOx Emissions-1 - Lower (moles/s)	2.10	0.80	1.30	1.50
Sat NOx Emissions-1 - Upper (moles/s)	4.80	3.10	3.40	3.50
Sat NOx Emissions-2 - Lower (moles/s)	1.70	1.10	1.20	1.30
Sat NOx Emissions-2 - Upper (moles/s)	5.20	2.70	3.50	3.70
NAEI Emission Rate (moles/s)	1.60	1.50	1.00	2.20

835

Source Name	Leeds	Bristol
Longitude	-1.55	-2.59
Latitude	53.80	51.46
Lon Edge - West	-1.69	-2.74
Lon Edge - East	-1.44	-2.47
Lat Edge - South	53.74	51.40
Lat Edge - North	53.86	51.55
Wind Speed Average (m/s)	8.70	7.20
Wind Speed Standard Deviation (m/s)	4.50	3.40
Wind Direction	S	E
E-Folding Distance (km)	207.00	123.00
Life Time (hr)	6.60	4.70
Life Time- Lower Wind (hr)	13.90	8.90
Life Time- Upper Wind (hr)	4.30	3.20
Satellite Emission Rate (moles/s)	5.70	3.80
Sat NOx Emissions-1 - Lower (moles/s)	3.70	2.50
Sat NOx Emissions-1 - Upper (moles/s)	7.60	5.10
Sat NOx Emissions-2 - Lower (moles/s)	2.70	2.00
Sat NOx Emissions-2 - Upper (moles/s)	8.60	5.50
NAEI Emission Rate (moles/s)	3.40	3.50

836
837